Industrial Chemistry & Materials

ROYAL SOCIETY OF CHEMISTRY

REVIEW

View Article Online
View Journal | View Issue

Cite this: *Ind. Chem. Mater.*, 2023, **1**, 595

Overview of CO_2 capture and electrolysis technology in molten salts: operational parameters and their effects

Qiuji Zhu,[a] Yimin Zeng*[b] and Ying Zheng *[a]

Received 30th January 2023,
Accepted 29th April 2023

DOI: 10.1039/d3im00011g

rsc.li/icm

Carbon capture and storage (CCS) technology is believed to be a promising solution for global CO_2 emission control and climate change. However, the application of CCS projects is facing a dilemma due to their negative cash flow. To address the challenge, it is critical to adopt an innovative technology that can capture and convert CO_2 simultaneously with satisfying efficiencies and can make a profit for the end users. Recently, molten salt CO_2 electrolysis that splits CO_2 into carbon and oxygen has been extensively studied. This study reviews the process mechanisms, the salt selection, and the effects of operating conditions, including temperature and voltage. In most reported articles, the CO_2 to carbon conversion efficiency reached at least 80%, and the current efficiency is over 90%, proving the promising potential of the molten salt CO_2 electrolysis method. Still, some aspects, such as the impurities' influences and electrode corrosion, have not been thoroughly investigated. Therefore, some suggestions are recommended for future work.

Keywords: CO_2 capture; CO_2 conversion; Molten salt CO_2 electrolysis; CO_2 reduction; Carbon nanotubes.

1 Introduction

1.1 CO_2 emission

The first recognition of the negative impact of CO_2 can be traced back to the 1870s when European scientists concluded that carbonic acid, a by-product of rapidly expanded industrialization, contributed to acid rain and artificial warming.[1] Later in 1936, lime scrubbing was first introduced to treat fuel gas, but this step was mainly targeted at the reduction of sulphur oxides.[2] The research focusing on CO_2 capture and separation was primarily initiated and driven by commercial interests, such as urea yield boosting, carbonated drinks, and most importantly enhanced oil recovery (EOR).[3,4] The CO_2 was sold at 50 USD per ton CO_2 for the EOR project, which essentially encouraged CO_2 capture.[5] There were over

[a] *Department of Chemical and Biochemical Engineering, Western University, London, Ontario, Canada. E-mail: Ying.zheng@uwo.ca*
[b] *Natural Resources Canada–CanmetMaterials, Hamilton, Ontario, Canada. E-mail: yimin.zeng@NRCan-RNCan.gc.ca*

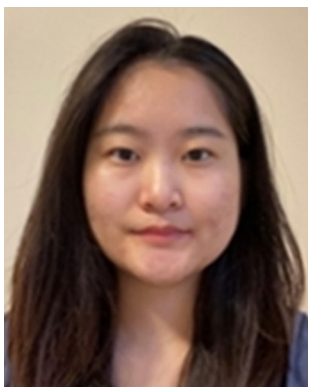

Qiuji Zhu

Qiuji Zhu is a Ph.D. student in the Department of Chemical and Biochemical Engineering at Western University. She graduated from the University of Saskatchewan. Her primary focus is using molten salts to capture and convert CO_2 released from power plants.

Yimin Zeng

Dr. Yimin Zeng is a leading research scientist at Natural Resources Canada (NRCan) CanmetMATERIALS, and also an adjunct professor at the University of Waterloo, Western University, and the University of Albert. His current research focuses on addressing materials technology and corrosion science challenges for the development and deployment of CO_2 capture, utilization and storage, advanced bioenergy production and application, next generation nuclear and thermal power systems, hydrogen energy, and decarbonation technologies in oil/gas industry.

140 EOR projects recorded in 2013, 88% of which were built in the USA.[3,4]

It is undeniable that carbon dioxide capture commercial programs are tied closely to both global and national political considerations and further, complicated by technological developments. The debates between the industry sectors and governments have been taking place for decades.[6,7] Since the 1970s, it has been witnessed that conferences and organizations increasingly promoted awareness of the harmful effects of CO_2 on all humankind and made countries collaborate to set up policies and projects.[8] Interestingly, the 1970s was also the year when the first CO_2 capture project applied for EOR, showing timeline overlaps between concepts and application developments.[3] The necessity of decarbonization and sustainability finally received special attention from policymakers and the public.

Carbon emissions are highly related to human activities. Thus, sorting out emission sources is the first step to adopting carbon capture projects. The pie chart in Fig. 1 provides a comprehensive breakdown of sectors contributing to global emissions. Energy-related sectors take the largest portion, 73.2%, where most energy used in this sector is supported by fuel combustion.[9] The trend of energy-related CO_2 emissions by fuel has kept increasing in the past 21 years, as shown in Fig. 2. In 2021, the greenhouse gas emission rose to another new peak, reaching a total of 40 Gt (gigatons) CO_2.[10] As coal-fired plants owned the cheapest operation cost, these plants guaranteed that coal was the leading fuel for energy generation and the top and stable CO_2 emission source. Oil and natural gas-related emission sources rebounded to 18.2 Gt, while coal emission sources reached a new-time peak of 15.3 Gt in 2021. The post-combustion is the most conventional and typical process in current thermal power plants. Although the CO_2 outlet level has a relatively lower concentration, only around 13 to 15%, post-combustion stands as a more competitive option because of finial considerations regarding technological barriers and costs.[11] Therefore, post-combustion CO_2 capture from power plants, especially coal-fired plants, has attracted substantial research interest. However, it is noticed that the Canadian Boundary Dam is, up to date, the only carbon capture and sequestration (CCS) project capturing post-combustion CO_2 from power generation.[12] The gap between the CCS project and research interests not only results from unmatured technologies but is also affected by the massive costs and investments.

Many countries throughout the world actively initiate applicable policies for CO_2 reduction and heavily invest in research programs as well as major industrial-scaled CO_2 capture initiatives. Norway, for example, is the first country that implemented the carbon tax and operated the first large-scale Sleipner CCS project, applying monoethanolamide (MEA) absorption to purify natural gas containing 9% CO_2.[3,13] Norway went through severe debates with the energy-intensive industry, revealing the complex impacts of the negotiated political economy on the project implementation.[7] The Norwegian Sleipner project inspired the birth of many other projects, such as Salah CO_2 Storage in Algeria in 2004 and the Snøhvit CO_2 Storage Project in Norway in 2008.[3] In 2014, Canada initiated the first industrial-scaled Boundary Dam CCS project in Saskatchewan to separate CO_2 from flue gases using amine absorption.[3,13] A fraction of the captured CO_2 was sold and applied to EOR, and the rest was stored *via* the Aquistore project in Saskatchewan.[14] The most recent CCS project, named Alberta Carbon Trunk Line, was built in Alberta, Canada, in 2020. MEA and methanol are used as absorbents to capture CO_2 from Sturgeon Refinery and Nutrient Redwater fertilizer plant.[15] According to Global CCS data, Canada has four commercial CCS projects, considering its high carbon tax of $50 per tonne of carbon dioxide equivalent emissions.[16]

Ying Zheng

Prof. Zheng is a full professor and a Canada Research Chair with the Department of Chemical and Biochemical Engineering at Western University. She is a Fellow of the Canadian Academy of Engineering and the Engineering Institute of Canada. Prof. Zheng is primarily interested in the field of Applied Catalysis for energy innovations. Her current research activities include CO_2 capture and utilization, converting CO_2 to chemicals, hydrogen production from waste, nitrogen fixation, bitumen and biofuel upgrade, and novel reactor design. She has developed several patented technologies that have been licensed or have licensing potential.

1.2 CO_2 capture & conversion methods

Several CO_2 capture methods have been proposed and validated in the past decades. Fig. 3 shows the typical classification of the carbon capture methods, including chemical absorption, adsorption, membrane separation, and calcium looping. Molten salt electrolysis, as an advanced method, can capture post-combustion flue gas and convert it into more valuable products to offset costs.

Amine absorption is the most mature and well-studied chemical absorption method for CO_2 capture.[17] Its application can be traced back to the 1930s.[2] Most industrial-scaled CO_2 capture plants, including the two post-combustion CO_2 capture plants operated at Boundary Dam and Petra Nova in Canada, employ the amine absorption method.[11,18,19] However, solvent regeneration requests elevated temperatures, which causes a vast energy penalty. In addition to energy consumption, the corrosivity and high volatility of amine solvents can cause various operational issues.[20–23] Adsorption

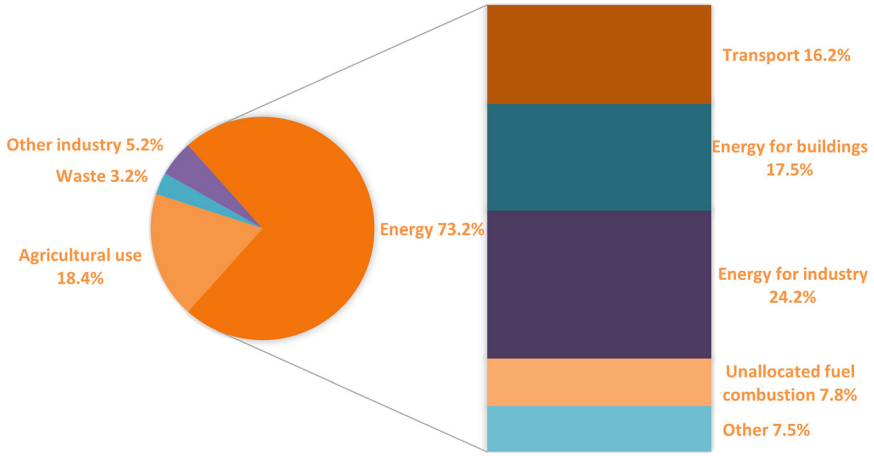

Fig. 1 Global greenhouse gas emissions by different industrial sectors with data collected from open-access ref. 9 with permission from Our World in Data, copyright 2020.

is another method that has been successfully applied in industrial-scale CO_2 capture plants, such as Air Products facilities for hydrogen production.[3,18] Natural sorbents, such as natural zeolites, natural plants (such as fruit shells), and coal-based materials, can be selected to perform adsorption, or human-made sorbents, such as activated carbon, metal–organic frameworks (MOFs), and zeolite, can adsorb CO_2.[24–26] So far, this pathway faces more challenges than absorption as the overall performance is even worse: high material costs (especially for MOFs), capacity loss during the process, high regeneration cost, and low adsorption capability (3–11 wt%), *etc.*[21] Other promising methods include membrane separation, calcium looping, and cryogenic separation.[25]

The above-mentioned conventional methods produce purified CO_2 and thus raise the same problem, which is the cost. The amount of purified CO_2 used for EOR and other industries is limited, and a large portion of captured CO_2 has to be stored, which leads to a negative cash flow. It explains the fact that there are only a few CCS projects, practically of which are funded by governments. Taking the Canadian Quest plant as an example, it requires average funding of 30 million annually for operation.[15] The Petra Nova project is another example, which captured the power plant's post-combustion CO_2 using amine absorption and sold for EOR. However, it was abruptly closed its business after only three years of operation due to imbalanced costs.[22] Due to its profit-driven nature, private corporations or even governments would only start to or continue operating CCS projects if they can generate profits and cover the cost of the carbon tax and other possible budgets.

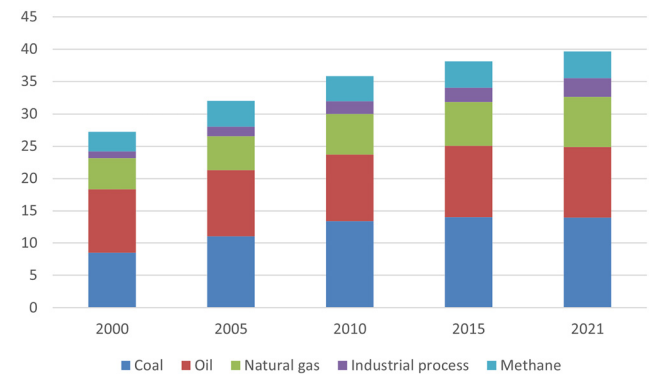

Fig. 2 Global energy-related CO_2 emissions by fuel types reproduced from open-access ref. 10 with permission from International Energy Agency, copyright 2022.

Numerous carbon conversion methods have been reported and well-studied.[23,27–30] A variety of conversion methods, such as photochemical, biological, and hydrogen transformation pathways, are being developed for industrial applications.[31–34] The advantage of these methods is that they can obtain hydrocarbons and other marketable products (such as dimethyl carbonate, synthesis gas, carboxylic acids, methane, *etc.*) that are significantly more valuable than pure CO_2. However, the deployment of these methods still faces critical challenges, such as evaporation occurring under high-temperature gas inlets, difficulty in final product separation, requirement on high CO_2 concentration feedstock. Moreover, some of the proposed methods likely suffer the unsatisfying production rates and the limitation of equilibrium and CO_2 solubility. For instance, the conversion of CO_2 to dimethyl carbonate was only around 1–5% due to the chemical equilibrium limitation.[23] It was also reported that the production using alkaline electrolytes, such as KOH, is restricted to the conversion of CO_2 to CO less than 50% due to the formation of carbonates and bicarbonates.[27]

Molten salt CO_2 electrolysis is a novel technology combining CO_2 capture and conversion. The development of the method was initiated in the 1960s and has quickly expanded since the 2000s. This method allows to capture CO_2 from hot flue gas, and the captured CO_2 can be directly converted in the molten salt electrolyte at high temperatures into valuable products, such as carbon, carbon monoxide, and O_2.[35] As CO production requires more energy consumption and presents lower current efficiency, CO would

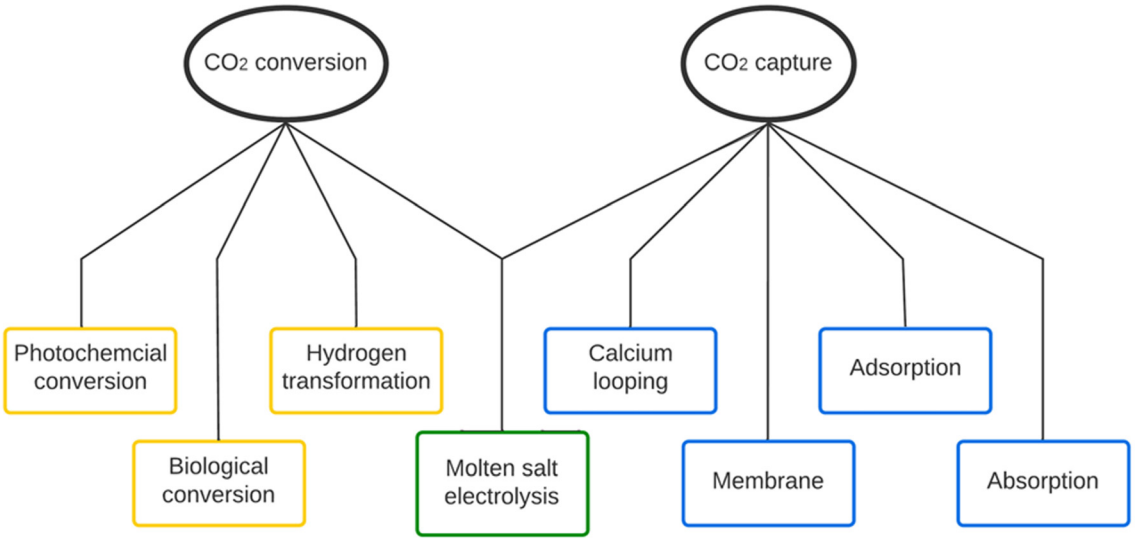

Fig. 3 General CO_2 capture methods developed.

not be an ideal product. Researchers show more interest in producing high-quality carbon materials and manipulating their nanostructures.

As its electrolyte contains zero water and targets carbon formation, molten salt electrolysis can result in a single solid carbon product with high current efficiency and avoid complex products with tough or multiple separations. Additionally, the *in situ* conversion of CO_2 to value-added products prevents extra costs after carbon capturing, such as CO_2 transportation costs, debatable and uncertain storing, maintenance costs, *etc.*[18,36] A molten salt CO_2 electrolysis plant is estimated to bring a net profit of $50 000 per ton of captured CO_2 for a power plant when the final electrolysis product is carbon nanotubes (CNTs).[37] One common approach for growing CNTs is chemical vapour deposition (CVD), which anticipates requiring at least 1440 MJ and emitting 28.55 kg CO_2e for producing one gram of CNTs,[38,39] Therefore, this profit and benefits can drive the molten method to potential scale-up plants and promote the carbon capture installed in general power plants, overweighing the financial burdens that the above-mentioned conventional methods have. This report will focus on this electrolysis method for carbon capture and conversion.

2 Molten salt CO_2 electrolysis system

Molten salt CO_2 electrolysis is used to capture CO_2 and electrochemically convert the captured CO_2 into valuable products, including solid carbon, oxygen, and carbon monoxide. The key components of the system contain electrolytes, electrodes, and an external power supply, as shown in Fig. 4. Electrolytes are melted salts containing zero water at a temperature higher or equal to melting points, and they are responsible for capturing inlet CO_2 and transferring ions and electrons. Product evolution and deposition occur on the electrode surfaces. In general, the inlet CO_2 is electrochemically split into oxygen and carbon or oxygen and carbon monoxide under harsher high-temperature conditions.

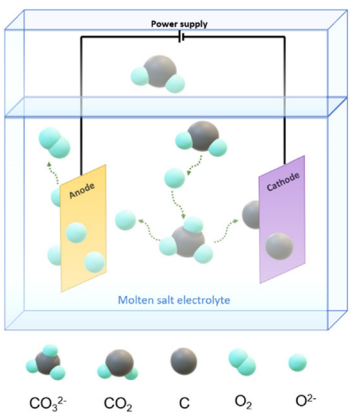

Capture: $CO_2 + O^{2-} \rightarrow CO_3^{2-}$

Cathode: $CO_3^{2-} + 4e^- \rightarrow C + 3O^{2-}$

Anode: $2O^{2-} \rightarrow O_2 + 4e^-$

Overall: $CO_2 \rightarrow C + O_2$

General temperature range: 400 – 900 °C

Electrolysis technique: constant voltage or constant current

Fig. 4 A schematic of a molten salt electrochemical system towards carbon deposition.

CO_2 is firstly absorbed by O^{2-} or CO_3^{2-} ions and turned into carbonate or dicarbonate ions. Then, CO_3^{2-} ions primarily follow a single-step reduction on the cathode through a 4-electron transfer, resulting in carbon deposition on the cathode and releasing oxygen ions. However, at higher temperatures, CO_3^{2-} ions tend to undergo a 2-electron transfer instead of a 4-electron to form CO as the final product on the cathode due to the fact that the generation of CO is more thermodynamically favourable than the formation of carbon. Note that the movement of carbonate ion is against the electric field since the reduction reaction exclusively happens on the cathode, and the driving force of concentration gradient overweighs the repulsion force of the electric field. The decreased carbonate ions at a cathode zone were reported in LSV tests, and the reduction of carbonate ions was found to weaken the electric current during constant voltage electrolysis. However, the effects of the electric field have never been reported nor compared to the concentration driving force. This topic should be investigated in the future to understand the cathodic electrolysis mechanism in a continuous operation.

The produced oxygen ions can either remain in the system to enhance CO_2 absorption or be oxidized as oxygen gas and then released from the anode. The whole electrolysis takes place in molten salt, which involves zero water. This can significantly avoid the competitive water split reaction. Thus, the current efficiency is improved and remains over 80%. Also, the formation of a complex hydrocarbon mixture is also avoided, so the product separation is much easier. As a result, the conversion of CO_2 to carbon and oxygen is more competitive as the current efficiency can exceed 90%.[40,41] However, when CO and oxygen are the desirable products, the process cannot achieve 90% carbon conversion at equal conditions. Thicker CO_2 inlet concentration (over 14%) and more extreme temperatures (at 900 °C) were required to push CO production to 90% conversion.[42] Additionally, the current efficiency for CO manufacturing purposes was relatively low, only around 36.9%, and this can be explained by unwanted side reactions.[42] More detailed mechanisms and reactions are discussed in the later section.

Table 1 lists the molten salt CO_2 electrolysis reported since 2019, and the records before 2019 can be found in Jiang's review.[62] Additionally, the generated records focus on the cases utilizing carbonate electrolytes, and the reasons will be discussed in detail in the electrolyte section. The trend between 2019 and 2022 can be classified into 3 major types:

Table 1 A list of molten salt CO2 electrolysis focusing on carbonates electrolytes since 2019

Electrolyte	T (°C)	Cathode	Anode	Current/current density	Carbon related products	Ref.
Li_2CO_3	770	Galvanized steel; Ni–Cr	Ni–Cr; galvanized steel	1 A	Multi-walled carbon nanotubes (MWCNTs)	49
Ta_2O_5–$CaCl_2$–CaO	650	Ni	Graphite	0.2–1 A cm^{-2}	Carbon particles	50
Li_2CO_3–Li_2O	770	Cu	Ir–Pt	0.2 A cm^{-2}	Carbon nano-onions; CNTs	51
Li_2CO_3–Li_2O–CaO–H_3BO_3	770	Muntz brass sheet	Nichrome sheet	0.2 A cm^{-2}	Carbon nanotubes (CNTs)	52
Li_2CO_3–Na_2CO_3–K_2CO_3–H_3BO_3	670	Muntz brass sheet	Inconel		CNTs	53
Li_2CO_3–Na_2CO_3–K_2CO_3	450–650	Ni	SnO_2	0.2–4 A g^{-1}	Activated carbons	54
KCl–LiCl; LiOH–NaOH; KOH–NaOH; Li_2CO_3–Na_2CO_3–K_2CO_3	225–475	Ti	Graphite		CO; hydrocarbons, H_2	47
Li_2CO_3–Li_2O	770	Muntz brass as	Inconel 718; Nichrome; Incoloy	0.5 A	Fe_3C; CNTs	55
LiCl–Li_2CO_3–$LiBO_2$	550	Ni	Graphite	25–100 mA cm^{-2}	CO	56
LiCl–Li_2CO_3–$LiBO_2$	550	Ni	Graphite		Carbon nanofibers (CNFs); CO	57
Li_2CO_3	730	Galvanized steel	Pt		Graphene; CNTs	43
Li_2CO_3–K_2CO_3–Na_2CO_3	650	NiO–Co_3O_4	$Ni_{10}Cu_{11}Fe$	10 mA cm^{-2}	NiCo@g-c powder	58
Li_2CO_3–K_2CO_3–Na_2CO_3	650–750	Ni	Pt	5–100 mA cm^{-2}	Graphite	59
MCO_3–Na_2CO_3–K_2CO_3 (M = Mg, Ca, Sr, and Ba)	710–850	Ni	$Ni_{10}Cu_{11}Fe$	3 V	Carbon particles	60
Li_2CO_3–K_2CO_3–Na_2CO_3	450	Ni	Pt–Ti	100 mA cm^{-2}	Electrolytic carbon	61
Li_2CO_3–Na_2CO_3	750	Brass	Inconel 718	200 mA cm^{-2}	CNTs	45
Li_2CO_3–Fe_2O_3; Li_2CO_3–Fe_2O_3–Ni	770	Muntz brass; Monel	Inconel 718; Nichrome; Inconel 600; Ni; Ir	8–600 mA cm^{-2}	CNTs	44
Li_2CO_3	750	Ni	SS	7.5 A	Carbon sphere	46
Li_2CO_3; Li_2CO_3–Na_2CO_3–K_2CO_3–LiOH; Li_2CO_3–$CaCO_3$–$BaCO_3$	450–750	Fe	Ni	10–450 mA cm^{-2}	CNTs; CO; H_2; CH_4	48

Note: this table includes reported molten salt electrolysis since 2019 and focuses on carbonate electrolytes. Reports prior to 2019 can be found in Jiang's review.[62]

1. Production of specific carbon nanostructure by modifying operation conditions and electrolysis system components;[43,44] 2. Method and equipment improvements, including separation improvement and reactor design;[45,46] 3. Expansion of molten salt CO_2 electrolysis to produce other materials, such as hydrocarbons.[47,48]

2.1 Electrochemical conversion mechanism

In a molten salt system, the reactions on the surface of electrodes are monitored closely *via* cyclic voltammetry (CV) measurements. At sufficiently high temperatures (a temperature higher than the melting points of selected salts), the desired electrochemical reactions for the carbon formation are shown below:[35,63]

$$\text{Cathode: } CO_3^{2-} + 4e^- \leftrightarrow C + 3O^{2-} \quad (1)$$

$$\text{Anode: } 2O^{2-} \leftrightarrow O_2 + 4e^- \quad (2)$$

Cyclic voltammetry (CV) tests are employed to record the reduction of CO_3^{2-} at a cathode, expressed in eqn (1).[35,64,65] As the peak of electric current declines quickly, there is deficient CO_3^{2-} reaching the cathode. Additionally, a slow scan linear sweep voltammetry (LSV) test measures the slow diffusion of oxide ions (O^{2-}).[64] The sluggish diffusions of CO_3^{2-} and O^{2-} limit the electrolysis.[64,66,67]

$$CO_2 + O^{2-} \leftrightarrow CO_3^{2-} \quad (3)$$

$$CO_3^{2-} + CO_2 \rightarrow C_2O_5^{2-} \quad (4)$$

Only at severe operating conditions, for example, at 1000 °C shown in Fig. 5, CO instead of carbon is produced due to lower Gibbs free energy for producing carbon.[67] Temperature is one of the critical factors. At a temperature exceeding 950 °C in molten Li_2CO_3, CO production is thermodynamically favoured over carbon deposition.[68,69] For instance, at 1200 °C in Li_2CO_3, the electrochemical potential, calculated from Gibbs free energy for carbon production, is about 1.1 V, while CO formation requires only 1.0 V.

$$CO_3^{2-} + 2e^- \leftrightarrow CO + 2O^{2-} \quad (5)$$

Side reactions have also been reported.[63,70] Kaplan documented the metal intercalation reaction since the carbon cathode swells while there are no visible changes to the graphite when used as the anode.[63] Tang observed the sparks resulting from alkaline metal and water during the sample wash, indicating the side reaction of metal deposition in eqn (6).[71] Cyclic voltammetry (CV) tests also reveal the two reduction peaks representing carbon and metal deposition, respectively, by eqn (1) and (6).[35,64,65] Heat deposition of carbonates is commonly observed, shown in eqn (7). Then, metal oxides can be ionic to also provide oxide ions for CO_2 capture in eqn (8). In order for eqn (8) to take place, metal oxides must be molten or dissolved in molten salts.

$$M^+ + e^- \leftrightarrow M \text{ (M = Li, Na, Ca or K)} \quad (6)$$

$$M_nCO_3 \leftrightarrow CO_2 + M_nO \quad (7)$$

$$M_nO \text{ (liquid)} = M^{N+} + O^{2-} \text{ (M = Li, Na, Ca or K)} \quad (8)$$

The formed metals can directly react with CO_2 gas to generate CO, as shown in eqn (9).

$$nM + CO_2 = CO + M_nO \text{ (M = Li, Na, Ca or K)} \quad (9)$$

When the temperature exceeds 850 °C, CO and CO_2 start to be co-produced. But if the applied current density or temperature is not high enough, the formed CO could be

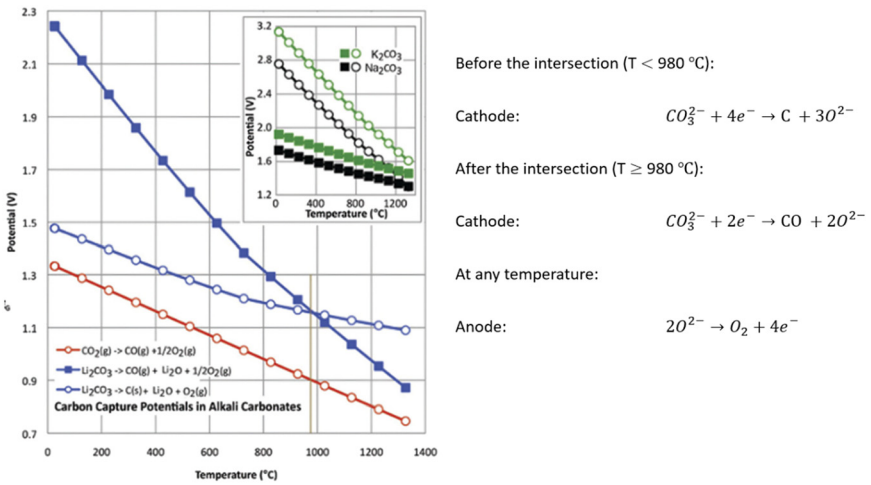

Fig. 5 Electrochemical conversion potential for carbon capture and conversion centra Li_2CO_3 (main figure), or Na_2CO_3 or K_2CO_3 (figure inset); in the inset, squares refer to $M_2CO_3 \rightarrow C + M_2O + O_2$ and circles to $M_2CO_3 \rightarrow CO + M_2O + \frac{1}{2} O_2$. To the right of the brown vertical line, CO is preferred. And C is preferred to the left of the line.[74]

decomposed to carbon and CO_2 *via* the Boudouard reaction.[63] If CO is the desired final product, molten salt electrolytes, such as LiCl–Li_2O, should be selected to avoid the Boudouard reaction.[67]

$$2CO \leftrightarrow CO_2 + C \quad (10)$$

Due to the reactions shown in eqn (1), (5), and (8), O^{2-} accumulates in the system and is then driven by an applied electric field to form oxygen on the anode surface. But if excessive O^{2-} is accumulated, it is possible to corrode alumina or zirconia container or electrode.[72] If carbon is used for the anode, excessive O^{2-} could react with the carbon to produce CO_2. Then, the carbon anode would degrade quickly.[41,63,67] Deposited carbon on the cathode also undergoes re-oxidation reactions with O^{2-}. In the cases of limited O^{2-} in molten chlorides, carbon could react with carbonate ions to re-produce CO_2.

$$C + nO^{2-} \leftrightarrow CO_n + 2ne^- \quad (n = 1 \text{ or } 2) \quad (11)$$

$$C + 2CO_3^{2-} \leftrightarrow 3CO_2 + 4e^- \quad (12)$$

Finally, the last step is to collect and/or wash the products. Carbon samples can be washed with water or acid solution, such as HCl, and the concentration of the acid can also affect the element composition of the final product. With a higher concentration of HCl, more impurities, including carbonates, oxides, and metals, in carbon samples can be washed away. For example, carbon samples obtained at the same operation conditions could have a maximum of about 13 weight% more carbon content. In comparison, around 9 weight% less oxygen when the sample is washed in 8.7 mol L^{-1} HCl compared to 2.3 mol L^{-1} HCl.[73]

Molten salt CO_2 capture and electrochemical transformation is a complex system. Thus, there is a list of parameters or components affecting the performance, products, energy consumption, *etc.* The parameters include cell components (electrolytes and electrodes), feeding stream, and operation conditions (power supply and temperature). In most cases, the carbon products are amorphous. A small number of impurities may also be identified depending on different operation conditions.[35,70,73] Therefore, carbons of different morphologies can be obtained by adjusting the operating conditions.

2.2 Electrolytes

In addition to molten salts, electrolytes can be replaced by aqueous solutions, ionic liquids, and solid electrolytes. Different electrolytes exhibit various selectivity, products, and efficiency. Electrolytes are crucial for collecting CO_2 from the incoming gas stream and transferring ions. Aqueous solutions are impractical when served as electrolytes due to a number of significant disadvantages, including poor electrochemical windows, water splitting, limited solubility, and slow reaction kinetics.[35,75] Ionic liquids show excellent chemical stability, high CO_2 solubility, and high conversion yield, but the high cost and low reaction kinetics hinder them from commercial-scaled applications.[35,76] Solid electrolytes have an overall higher current efficiency, but their specific conductivity is less than half that of molten salt electrolytes.[62] Even worse, sulphur impurities negatively affect the solid electrolytes, making this type of electrolytes unfavoured for capturing power plant flue gas commonly containing sulphur compounds.[62]

Many researchers believe high-temperature molten salts are the optimal electrolyte because of their satisfying properties. Molten salts present low toxicity, high heat capacity, wide electrochemical operating window, high ionic conductivity, and low costs due to abundant availability.[77] Furthermore, the same metal oxide components, for example, Li_2O, show an enhanced CO_2 absorption ability in the molten phase compared to the solid phase.[78] Impurities from flue gas, SO_2 and NO_2, can be converted into valuable S/N-doped carbon materials.[78,79] Selecting a molten salt electrolyte is considered more crucial than choosing an electrode since electrolytes have a greater impact on the final carbon product. Wang observed that carbonates and oxides impacted the nanostructures of resulted carbon, while five different cathodes produced little changes to the final product.[80]

Carbonates, chlorides, and oxides containing Li^+, Ca^{2+}, Na^{2+}, and K^+ are the most widely researched electrolytes due to their wide electrochemical windows and good CO_2 solubility.[62] Carbonates and chlorides take up a large portion of salts, and oxides are commonly used as additives, ranging from 1 wt% to 30 wt%. The types of salts present distinct advantages and drawbacks, and as a result, they are commonly mixed together to achieve optimal performance, such as lower melting points. But before mixing, it is essential to identify the features of salts first.

2.2.1 Carbonates or chlorides. Mixed salts frequently present lower melting temperatures than pure constituents. Chlorides show even lower melting points than carbonates. LiCl–KCl eutectic is 353 °C, lower than general carbonates listed in Table 2.[81] However, it should be noted that operating temperatures are not the only factor contributing to total energy consumption, as voltage supply also take a large portion of energy input. With higher temperatures, the voltage requirement for the reaction is reduced. For instance, the energy consumption is 16.3 kW h kg^{-1} of carbon

Table 2 Melting points of carbonates and their mixtures[83]

Salt system	Melting point (°C)
Li_2CO_3	723
Na_2CO_3	854
K_2CO_3	891
Li_2CO_3–Na_2CO_3 (52–48 mol%)	501
Li_2CO_3–K_2CO_3 (62–38 mol%)	498
Na_2CO_3–K_2CO_3 (56–44 mol%)	710
Li_2CO_3–Na_2CO_3–K_2CO_3 (43.5–31.5–25 mol%)	397
K_2CO_3–$MgCO_3$ (57–43 mol%)	460

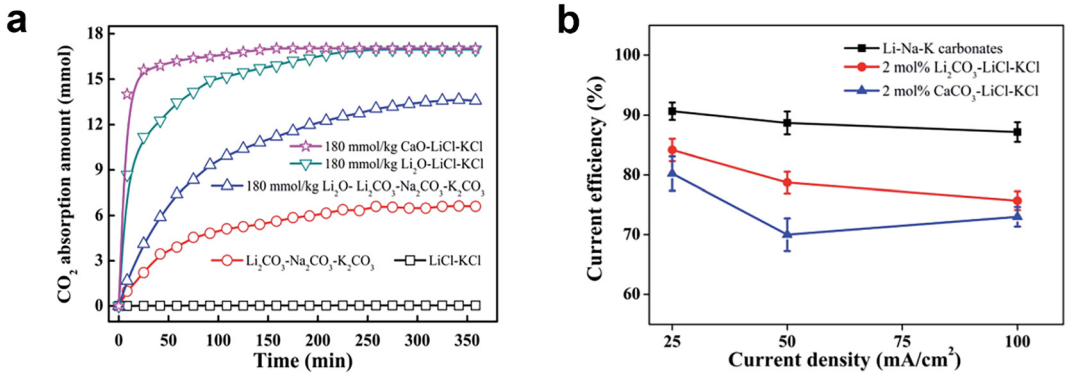

Fig. 6 (a) CO_2 absorption curves in different molten salts at 450 °C with the CO_2 partial pressure of 50 kPa; (b) current efficiency for galvanostatic electrolysis in different molten salts under CO_2 atmosphere at 450 °C.[76]

produced at 650 °C but 31.4 kW h kg^{-1} at 450 °C.[81] CO_2 solubility in chlorides is extremely low, resulting in low mass transfer.[82] As shown in Fig. 6, molten chlorides like LiCl–KCl have poor CO_2 absorption. Thus, chlorides need to team with oxides or carbonates to improve carbon absorption and conversion. Compared to carbonate electrolytes with oxide additives, the chlorides with oxide additives show faster CO_2 absorption and reach equilibrium within 2 h, which demonstrates a better CO_2 absorption. The reaction of Li_2O and CO_2 resulting in Li_2CO_3 is responsible for the high absorption capacity. The conversion efficiency for Li_2O into Li_2CO_3 almost doubled in molten chloride electrolyte (around 94%) compared to that in molten carbonate electrolyte (about 45%), indicating the molten salt composition affects both the absorption thermodynamics and the kinetics for Li_2O conversion.[76] This change in the oxide conversion efficiency can be explained by the low activity of Li_2O in the molten carbonates and the strong chemical interaction between CO_2 and carbonates. The latter slows down the CO_2 diffusion rate for desired conversion reactions.

Another difference between carbonates and chlorides is the solubility of additives, such as CaO and Li_2O, which later lead to different reaction mechanisms. CaO or Li_2O is soluble in $CaCl_2$ but hardly dissolves in carbonates.[78,81,84] Chloride electrolytes typically contain oxide additives. However, they still have overall fewer oxygen ions than carbonate electrolytes, which can reduce the adverse effects of the consumption of deposited carbon as indicated in eqn (11) and (12).[41] However, when CO_3^{2-} is wholly consumed in chlorides, the current density reaches nearly zero.[81] It indicates neither pure chlorides are suitable for CO_2 splitting, nor chlorides with additives are stable for long-term electrolysis. A more detailed and comprehensive review focusing on chloride salts can be found in Díez's report, including how the salts and added biomass serve as templates for the formation of micro-pores, which resulted in various carbon nanostructures.[85]

For carbonate electrolytes, the solubility of its oxide or additives leads to two different mechanisms. For insoluble oxides (such as CaO), the primary electrolysis reaction refers to the conversion of carbonates ($CaCO_3$) into corresponding oxides (CaO) and carbon deposition, and O_2 formation.[60] Solid CaO on the cathode surface is difficult to absorb CO_2 and convert itself back into molten $CaCO_3$ to complete the loop.[86] Therefore, carbonates, whose oxides are insoluble, keep being consumed over time at high operation temperatures, and the oxides and carbon co-deposit on the cathode surface.[60] The other mechanism is for soluble oxides (such as BaO), where carbonate ions are converted to carbon and O_2. In this case, BaO dissolves in the electrolyte and provides oxide ions to continuously capture CO_2 and transfer back to fresh $BaCO_3$. Only carbon deposits on the cathode surface. Similar discoveries are observed where CaO and Li_2O solidify and cover cathodes, hindering CO_2 absorption and weakening electrolysis.[66,81]

Kanai *et al.* are among the few research groups investigating the mass transfer in molten carbonates, as shown in Fig. 7. Elevated temperature enhanced CO_2 solubility in both binary (Li–K) and ternary (Li–K–Na) molten carbonates, and the solubility values of these two types of carbonates are close to each other. The dissolution of CO_2 in molten salts can be classified into two categories: physical and chemical dissolution. The chemical dissolution is expressed in eqn (3) and (4) while the physical dissolution is

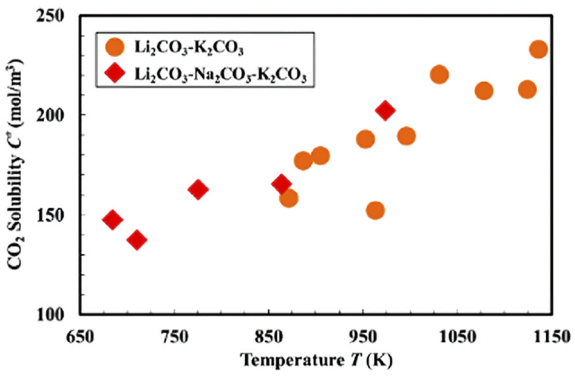

Fig. 7 CO_2 solubility in molten carbonates at different temperatures at 1.01×10^5 Pa.[87]

Table 3 Characterization of carbon produced in different molten salts using Raman and nitrogen adsorption–desorption tests at 50 mA cm^{-2} (ref. 76)

Molten salt	$I_D:I_G$	S_{BET} (m^2 g^{-1})	Pore volume (cm^3 g^{-1})	Average pore size (nm)
Li_2CO_3–Na_2CO_3–K_2CO_3	0.86	897.4	0.862	4.62
2 mol% Li_2CO_3–LiCI–KCI	0.67	113.9	0.279	9.97
2 mol% Ca_2CO_3–LiCI–KCI	0.72	157.9	0.125	3.98

presented in eqn (13), estimated at 2% of the total dissolved CO_2.[58,87] Therefore, it is believed that chemical dissolution dominates CO_2 solubility. At 700 °C, the ratio of chemical to physical dissolution is 98%: 2% in ternary (Li–K–Na) molten carbonates.[88,89] This ratio again indicates the necessity of oxides additives in chloride electrolytes and explains why the solubility of different types of carbonates is similar.

$$-\ln C^*RT = NA\gamma/RT \quad (13)$$

(C^* is CO_2 solubility, R is the gas constant, T is temperature, N is Avogadro's number, A is the contacting surface area, and γ is the surface tension of the molten salts).

Fig. 6 shows that molten carbonates also have higher current efficiency at the same current rate, indicating that using carbonates could prevent several side reactions that occur with chlorides, particularly the development of chlorine gas.

Electrolyte compositions can significantly affect the properties of produced carbon in terms of morphology, surface area, pore volume, and conductivity. In Table 3, Deng's research shows that the specific surface area and pore volume of carbon obtained from molten carbonates can be 8 times larger than those from molten chlorides.[76] As discussed above, carbonates also hold more remarkable absorption ability and stability. These essential characteristics outweigh their drawbacks, which lead to favouring carbonates over chlorides in molten salt electrolysis. Therefore, the cation selections section focuses on carbonate salts and their related research.

2.2.2 Cation selections. The choice of alkaline metal cations has a considerable impact on the reaction and end products, in addition to the broad types between carbonates and chlorides, due to their thermodynamic characteristics and cation sizes. The following discussion mainly focuses on carbonate electrolytes. Metal cations dominate the properties in the carbonate system and can be reduced to metal elements during electrolysis. Metal deposition has a contradictory influence on electrolysis. On the positive side, metal particles can act as active sites for carbon deposition. However, metal deposition generally requires more energy input and sacrifices current efficiency. Li or Ca carbonates are more stable and suitable than Na or K-containing carbonates, considering the deposition potentials, heat decomposition, and quality of carbon produces. Furthermore, Li, Ca, and Ba metal depositions require more challenging conditions than Na or K. Carbon deposition is less difficult in Li, Ca, and Ba carbonates than in Na or K carbonates, as shown in Table 4.[34,60] Li_2CO_3 conductivity is 6 S cm^{-1}, 2 times higher than Na_2CO_3 and 3 times higher than K_2CO_3 at their melting points.[74] Its higher conductivity lowers ohmic loss and thus enhances reactant or electron mass transfer. Thanks to various properties, a mixture of carbonates containing different cations is commonly applied to offer optimum behaviour.

Li_2CO_3 can decompose at temperatures far lower than the melting point, while $CaCO_3$ is chemically stable as its decomposition temperature exceeds its melting point (825 °C).[41] As previously discussed, temperatures over 825 °C are more favourable for CO generation than carbon production. Under the same operating conditions, the CO_2 capture percentage in $CaCl_2$–CaO can be approximately 17 times higher than in LiCl–Li_2O because Ca has higher reduction energy thermodynamically than Li does.[67] The relatively low conductivity of $BaCO_3$ and low basicity of BaO can improve the cell voltage during electrolysis and limit anode corrosion.[90] But $BaCO_3$ is an uncommon option due to its high cost and toxicity.[41]

Different cations in carbonates also lead to various carbon nanostructures. Li^+ and Ba^{2+} are expected to promote the formation of CNTs, but K^+ hinders the formation of carbon nanostructures.[80,91] It is further evidence that electrolytes containing more than 50 wt% of Na or more than 30 wt% K carbonates inhibited CNTs growth but supported the development of carbon nano-scaffolds (CNS).[53] Overall, previous studies supported lithium-related salts because of their exceptional qualities.

2.2.3 Additives. The additions have been used to fine-tune carbon nanostructures and improve CO_2 absorption. The additives can be classified into two groups: carbonate heat decomposition (CaO, Li_2O, and BaO) and foreign ones (CuO, CoO, ZnO, Fe_2O_3/Fe_3O_4, *etc.*). The additives that have been well studied include CaO, Li_2O, CuO, CoO, ZnO, and Fe_2O_3/Fe_3O_4.[81,92] Metal cations of the additives can serve as nucleation sites and influence the nanostructures of carbon and improve the CO_2 capture rate due to chemical bonding between acidic CO_2 and alkaline absorbents.[76] However, the overall CO_2 capture and conversion efficiency may not

Table 4 Deposition (*vs.* CO_3^{2-}/CO_2–O_2) of alkali and alkaline earth metals *via* eqn (7)–(8) and carbon *via* eqn (1) at 600 °C (ref. 41)

Molten salt	Alkali metal (V)	Carbon (V)
Li_2CO_3	−2.964	−1.719
Na_2CO_3	−2.546	−2.551
K_2CO_3	−2.612	−3.083
$CaCO_3$	−3.033	−1.349
$BaCO_3$	−3.069	−1.992

enhance, considering the complex effects of oxide ions in metal oxide additives.[64,69,83]

When Li_2CO_3, $CaCO_3$ or $BaCO_3$ are used, Li_2O, CaO, and BaO are formed as thermal decomposed products. For instance, 1 mol Li_2CO_3 could generate up to 0.0222 mol Li_2O at 750 °C in the air without the influence of electrochemical reactions.[80] As shown in Table 4, the voltage required to reduce sodium ions to sodium is close to that required to deposit carbon. Since potassium deposition potential is lower than carbon deposition potential in molten K_2CO_3, a large portion of electrolysis current would be wasted on reducing potassium if carbon is the desired product. This also suggests the loss of electrolytes when metals deposit on the cathode. Li_2O, as a decomposed product or a manual additive, serves as an intermediate for capturing CO_2, ensuring continuous operation, and avoiding wasting current on undesired metal deposition. Because Li_2CO_3 holds a relatively low potential for carbon deposition and a high potential for metal deposition, Li_2O can continuously absorb carbon dioxide and form Li_2CO_3, and regenerate oxides after carbon deposits. In this continuous operation, Li_2O is stable as it can avoid being reduced to Li metal as long as the electrochemical window is wisely chosen. Thus, in case Li_2CO_3 is selected as the electrolyte, carbon would be produced without deposition of metal Li so that the molten salt system remains stable and continuous addition of salts is avoided. This viewpoint was supported by the experimental results that the alkalinity of molten salt Li_2CO_3–Na_2CO_3–K_2CO_3 remained steady during continuous operations, and no Li_2O accumulation could be achieved in the system.[35] Furthermore, Li^+ is a critical component for molten salt electrolysis carbon deposition. Tests on CV performed to track the peaks in carbon reduction provide evidence for this claim. Without Li_2CO_3, the Na_2CO_3–K_2CO_3 electrolysis experiment showed no carbon reduction peak at 750 °C. Adding more CaO enhanced CO_2 absorption with a linear correlation of about 1 between metal oxides and CO_2.[81] However, this conversion was reduced by 20% when the temperature increased from 550 to 600 °C because the carbonation formation is exothermic, which is not favoured at a higher temperature. Li_2O was also observed to absorb more CO_2 with increasing weight percentage, and the optimum trial reached a maximum of 0.1105 g_{CO_2} g_{melt}^{-1}, conducted with 8 wt% additive at 923 K under 101.3 kPa.[93] However, it should be highlighted that these gas solubility data was obtained without electrolysis, and section 2.2.1 and below contents discuss how metal oxide additives solidify on the cathode and hinder absorption due to additives' poor solubility in electrolytes.

Foreign metal oxides serve as necessary nucleation sites for special carbon nanostructure growths, especially CNTs growth. In fact, one of the most popular research topics focuses on molten salt carbon dioxide capture and electrolysis to produce CNTs and other special nanostructures shown in Fig. 8. Various metal oxides have been tested and examined for carbon nanostructures. Zn or ZnO additives were favourable for carbon nanofiber formation.[92] Fe_2O_3 is another popular additive. In some cases, the electrodes contain transition metals that can be reduced to metal elements during electrolysis.[44,55] These transition metals helped the growth of the tip, and the end of a CNT as TEM HAADF showed evidence of metal inside CNT and the two ends.[44] Another interesting case is that Fe ions could successfully combine with produced carbon to synthesize MWCNT/Fe_3C nanomaterial at 900 °C under 3.1 V with iron melt in the electrolytes.[94] GeO_2 is another example.[95] Soluble GeO_2 was electrochemically reduced to Ge and deposited on the cathode with carbon, and during this process, Ge anchored on the ends and the inner wall of formed carbon to grow carbon nanotubes. Considering Chen's proposed theories about how additives' solubility affects reaction mechanisms using CaO and BaO, the key

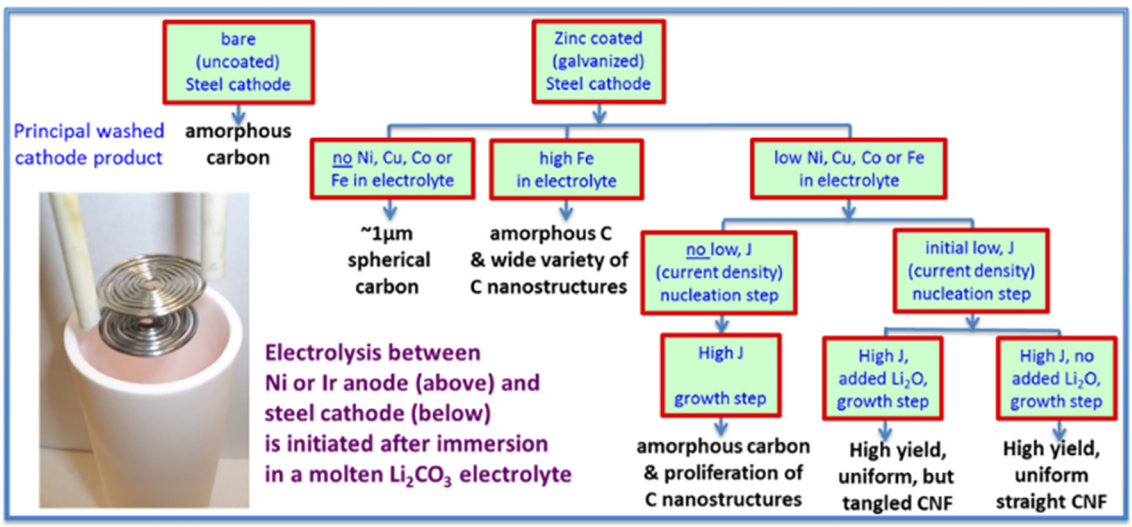

Fig. 8 Molten carbonate electrolysis pathways converting CO_2 leading to high yield, uniform CNF product.[92]

factor for CNTs formation may depend on the solubility of additives in electrolytes. Overall, one possible theory is that metal oxide additives are reduced to metal and then serve as the active sites for the formation of carbon nanotubes or nanofibers.[44,55,92,94,95]

In addition to metal, oxygen ions in these additives need to be examined since they play a significant role in the splitting reaction and regulate the rates of many reactions, such as the evolution of oxygen on the anode surface and the conversion of CO_2 to CO_3^{2-}. Therefore, there exists an optimal quantity of additives that should be applied to each system. Metal oxides are crucial for supplying oxygen ions when molten chlorides are applied as electrolytes. There is no carbon deposition detected in the absence of metal oxide additives.[78] The metal oxide additives enable not only to capture CO_2 and to initiate the subsequent carbon deposition but also to introduce significant defects into final carbon products (*e.g.* CNT),[41,80,83] The introduction of over-dosed O^{2-} has a drawback on CNTs formation. 30 wt% BaO with 0.04 wt% Fe_2O_3 and 0.04 wt% Cr_2O_3 additives led to 20% CNTs yield, which was about 10% higher than 7.1 wt% BaO but 60% less than using 0.1 wt% of Fe_2O_3. Deng reported that the CaO additive was solidified and covered the cathode when O^{2-} was over-dosed.[81] As shown in eqn (1), the electrolysis of carbonate ions produces 3 units of oxide ions. These oxide ions near the cathode can easily bond with metal cations to form metal oxides. Solidified CaO showed poor CO_2 absorption, and the covered cathode lost activity. Moyer *et al.* also reported that Li_2O build-up at the cathode lowered the reaction and decreased the carbon graphitization degree.[66] Gao's article provides another explanation that external O^{2-} from dissolved oxide additives lowers the O^{2-} concentration gradient in the electrolyte, and thus it slows the diffusion and limits the electrolysis rate.[64] Additional research must be conducted to fully comprehend.

Therefore, researchers also attempted to manage oxygen ion products and continuously remove them instead of increasing oxygen ions in the system to capture CO_2. Yet $LiBO_2$ has been reported to be an effective additive. BO_2^- acts as an O^{2-} absorbent and converts into BO_3^{3-}, which later reacts with CO_2 to produce CO_3^{2-} and BO_2^-.[57] The CO_2 concentration was reduced from 14% to 7%. The $LiBO_2$ free electrolytes presented a CO_2 concentration drop of 2.1%, only one-third of the concentration drop in $LiBO_2$ electrolyte.[57] The reduction potential was reduced by 400 mV in this attempt, which resulted in a lower applied voltage at the same current density and a 60% reduction in energy consumption.

2.3 Electrodes

The two crucial elements in this electrolysis system are the anode and cathode, which are responsible for oxygen evolution and carbon deposits, respectively. Therefore, the anode must promote oxygen generation, while the cathode should have active areas for particular carbon nanostructures. Both electrodes nonetheless share some characteristics in common, such as resistance to corrosion in hostile situations with molten salts.

Through the CO_2 splitting reaction, the changes on electrodes cause current fluctuation and unstable performance; thus, it is important to avoid corrosion due to molten salts or oxygen evolution effects on electrodes. Corrosion of carbonates can even dissolve the alumina or zirconia container.[72] Corrosion easily alters electrode surface and compositions. When the effective anode area significantly decreases, the current density can have a 66% drop.[67] While formed carbon expanded on the cathode surface, the current density increased.[81] Even when the used Ni electrode seemed unchanged, as observed by eyes, the green residue in the electrolyte indicated part of Ni was oxidized and escaped.[96] More stable metals, alloys or oxides should be utilized to minimize corrosion, such as NiCr alloy and TiO_2.

2.3.1 Cathode. Metals, alloys, metal oxides, and carbon-based materials are the different categories of cathode materials. Among these, metals are the favourite choice as it is believed that metal particles decide carbon nanostructure types based on density functional theory.[97] Fig. 8 illustrates how cathode materials determine the composition of the final carbon products. A metallic component in the cathode can be reduced to metal particles in the system. Nanoscale metallic impurities found in the carbon framework indicate that metal works as a catalyst in the system.[98] Based on this mechanism, cathode material can be engineered to insert specific metallic layers in the formed carbon products. For example, Cr–O can be inserted to form a Cr–O–C interlayer at 700 °C under 2.8 V.[99] But the metal selection is limited to the ones that do not have a strong catalysing effect on the Boudouard reaction.[72] In general, Fe, Ni, Ti, Mo, Pt, their metal oxides, and alloys are widely used as the cathode in molten salt CO_2 capture.

Iron is earth-abundant, affordable metal and has incredible influences on carbon products. During electrolysis, a stainless steel cathode releases Fe and other alloying metals, including Ni and Cu.[100] These ions result in a micro explosion and help form graphene when CO is produced. Douglas's research group manipulated the CNTs sizes by adjusting Fe sizes, as shown in Fig. 9.[101]

In addition to Fe, a copper cathode enhances the formation of a unique ball structure of graphene, while a nickel cathode leads to flat graphene sheets. The various carbon nanostructures indicate the active metal atoms on the cathode act as the nucleation sites and catalyse the development of carbon films.[100] Ti is another suitable material as Ti is chemically stable in molten salts, and the formed oxide layer, TiO_2 or $LiTiO_2$, is also conductive and insoluble up to 900 °C in Li_2CO_3 and Li_2O.[72] Zn is another case of how cathode metal alters carbon nanostructures. Zn galvanized steel cathode surface generates a high percentage (over 80%) of carbon nanofibers, which cannot be achieved by using 316 stain steel cathode.[92] One way to explain these

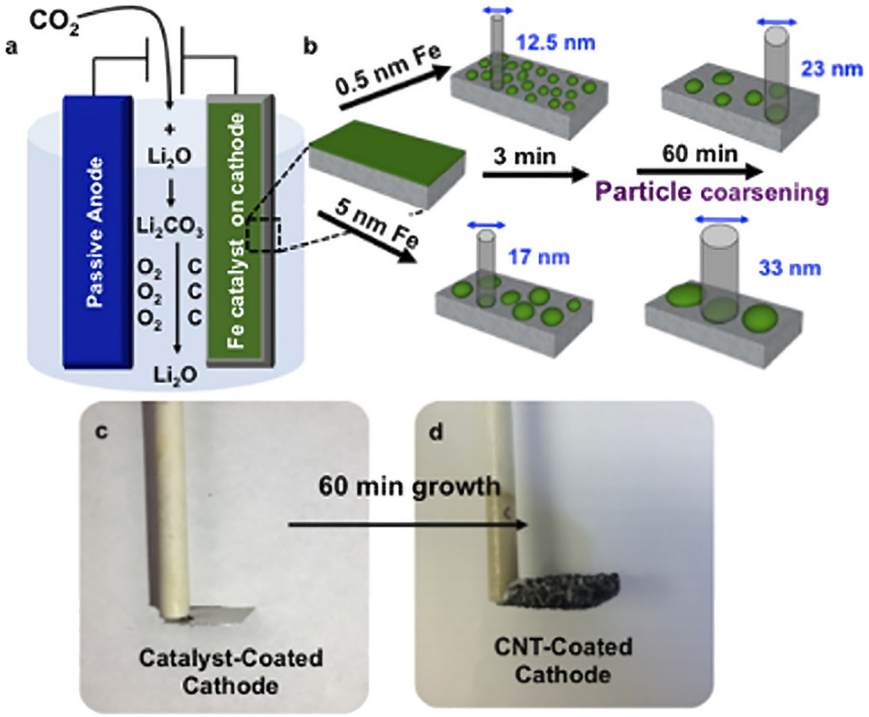

Fig. 9 Schematic illustrations: (a) electrolysis setup, (b) catalyst of varying thickness and growth time controlling the CNT diameters, (c) catalyst-coated stainless-steel cathode before, (d) after 60 min growth of CNTs.[101]

experimental observations can be through the density functional theory.[97] It showed that the π–d bond between the metal particles and nanotubes encouraged the nanotube growth, and the overlap of the d orbitals from Zn and Ni could improve the nanotube quality.[97] However, the interaction of oxygen ions and metals was not considered, including the formation of metal oxides and the solubility of metals and metal oxides.

Graphite is not a good cathode choice as it quickly swells and decomposes due to electrolyte metal intercalation, even under a low cathode current of 30 mA cm^{-2}.[72] Additionally, the CV scanning results showed that carbon triple bonds were electrochemically converted into carbon, which is more difficult on graphite than metals such as Ni.[102]

2.3.2 Anode. O^{2-} ions diffuse through the molten salt and accumulate on the anode to produce oxygen gas. O_2 concentration was measured to increase by about 10 mol% comparing the effluent gas before and during electrolysis, as presented in Fig. 10(b).[72] The anode is responsible for catalysing oxygen generation and avoiding accumulating O^{2-}. Removing O^{2-} timely from the molten salts ensures the required electrical current for carbon deposition.[67] As O^{2-} ions do not exist freely in the electrolyte; they bond with carbon dioxide or metal ions to form carbonate ions and metal oxides. It is commonly believed that the diffusion of oxygen ions (or carbonates ions and metal oxides) is the rate-determining step.[57,64,65,81] Because of the unique sluggish diffusion, the concentration of outlet oxygen gradually

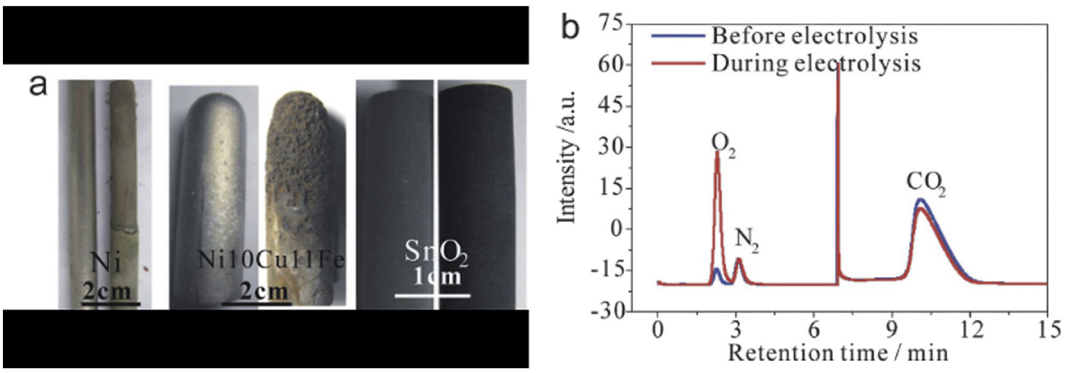

Fig. 10 (a) Digital photos of Ni, $Ni_{10}Cu_{11}Fe$ and SnO_2 electrodes before and after serving as the anode; (b) gas chromatograms of the outlet gas before and during electrolysis using the SnO_2 anode.[35]

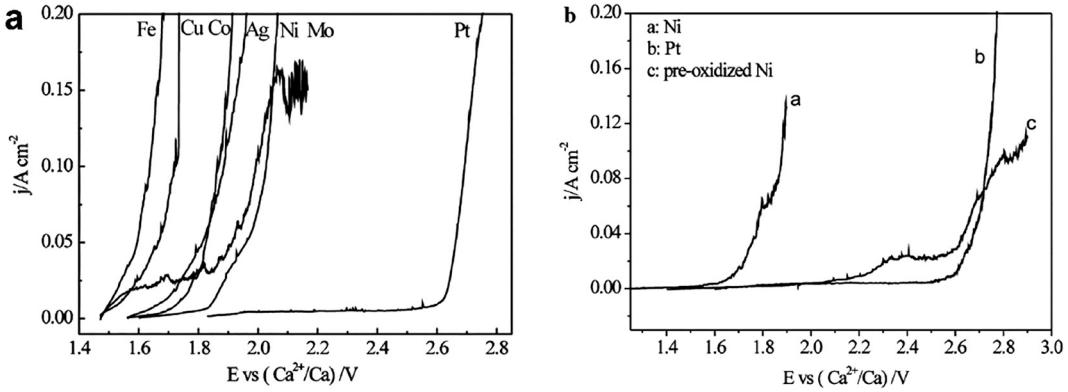

Fig. 11 (a) Polarization curves of metals in molten $CaCl_2$ – 2.5 mol% CaO at 850 °C (potential scan rate, 2 mV s^{-1}); (b) polarization curves of Ni, Pt and pre-oxidized Ni in molten $CaCl_2$ at 850 °C (potential scan rate, 2 mV s^{-1}).[103]

increases over electrolysis time.[60] At the same time, the materials should also be robust enough to resist oxidation in the long run. Anode material can also be classified into metals, alloys, metal oxides, and carbon materials. The common materials are Pt, Ni, NiO, Ni-based alloy, and SnO_2. Developing suitable anode materials has always been a significant challenge and research hotspot, especially when the effectivity of cathode materials is controversial due to carbon deposition.

Metals own satisfying conductivity, but their poor durability seriously limits their applications. The anodic dissolution order of metals in molten $CaCl_2$–CaO was Fe, Cu, Co, Ag, Ni, Mo, and Pt, shown in Fig. 11. A higher polarization current density at a potential indicates the dissolution of such metal is faster. Thus, Pt has outstanding stability among all these pure metals. Pt's superior performance was proved again in the anodic polarization curve in molten Li_2CO_3–Na_2CO_3–K_2CO_3. However, the high price of this noble metal hinders its real-world application.

Metal oxides were investigated as anode materials, targeting high corrosion resistance and lower prices compared to Pt. Ni is of great interest to scientists because it naturally generates a NiO top surface layer with more resistance.[92] Fig. 11(b) shows NiO could have comparable resistivity to Pt. Other Ni-containing materials, such as $_{(1-x)}CaTiO_3$–xNi, have been studied. Among them, $_{0.5}CaTiO_3$–$_{0.5}$Ni and $_{0.4}CaTiO_3$–$_{0.6}$Ni materials present satisfying anodic and stable performance with a corrosion rate of 4.958×10^{-3} g cm^{-2} h^{-1}.[104] However, Du *et al.* pointed out that temperature played an important role in influencing the formation of a Ni oxidized layer on the Ni anode. At a temperature lower than 575 °C, $Li_xNi_{1-x}O$ was the main oxidization product, which is soluble in the carbonate electrolytes. Only at temperatures above 575 °C could an evenly distributed, insoluble, and robust NiO layer form, which could shield the anode from further oxidation.

Other metal oxides also show a positive possibility of being applied as an anode, including SnO_2, RuO_2–TiO_2, and Ti_4O_7. Among the mentioned metal oxides, the SnO_2 anode shows similar polarization curves compared to Pt and Ir and becomes a popular anode choice.[35] Fig. 10(a) presents the photos of a SnO_2 electrode before and after the electrolysis, where no obvious mass loss is observed. In an extreme case of 500 hours electrolysis, the SnO_2 anode lost less than 0.1 wt%.[35] However, the polarization curve slopes of SnO_2 are less significant than those of Pt and Ir, indicating the oxide has a worse oxygen evolution activity on SnO_2.[105] RuO_2–TiO_2 was employed in molten chlorides, and there were no physical changes observed after a 4 hour operation.[106] But Ru is also a noble metal on Earth, and Ti oxides lack stability compared to other oxides.[105] Additionally, there is a lack of records for RuO_2–TiO_2 performances in molten carbonates.

Alloys can also be promising anode materials thanks to their satisfying properties. Compared to metal oxides, alloys have better conductivity and malleability; alloys also show better corrosion resistance compared to pure metals. Ni-based alloys are the most popular anodes used in carbonate electrolytes.[49,58,60,91,101,104] Ni alloy can have two roles based on different metal atoms: a NiO layer as a protective layer is formed during the electrolysis. In contrast, other metal particles in the alloy are believed to catalyse different carbon nanostructures. $Ni_{10}Cu_{11}Fe$ is one example of this alloy strategy. By observing with eyes, the oxidized layer of NiO occurred on the anode surface due to the specific green colour of NiO, different from other oxides or metals, but there was no dimension change of the anode observed after over 100 hours electrolysis.[60] Another case for Ni alloy is Ni–Cr alloy, where NiO is still the leading protective layer against corrosion.[49] Cr_2O_3, the oxide form of Cr in the alloy, cannot be detected, which again indicates NiO acts as the protective layer and remains during the electrolysis.[49] Besides the protective surface strategies, other types of alloys are applied to investigate the effects of metal particles on carbon nanostructures. Fe materials were also tested previously for anode performances. Incoloy, an Iron-based alloy with over 40% iron content, released Fe ions into the system when it was used as an anode.[55] Because the iron content is large in Incoloy, the released Fe ion amount was significant, which combined with carbon and formed iron carbide on the CNTs external walls, resulting in a magnetic carbon material.[55]

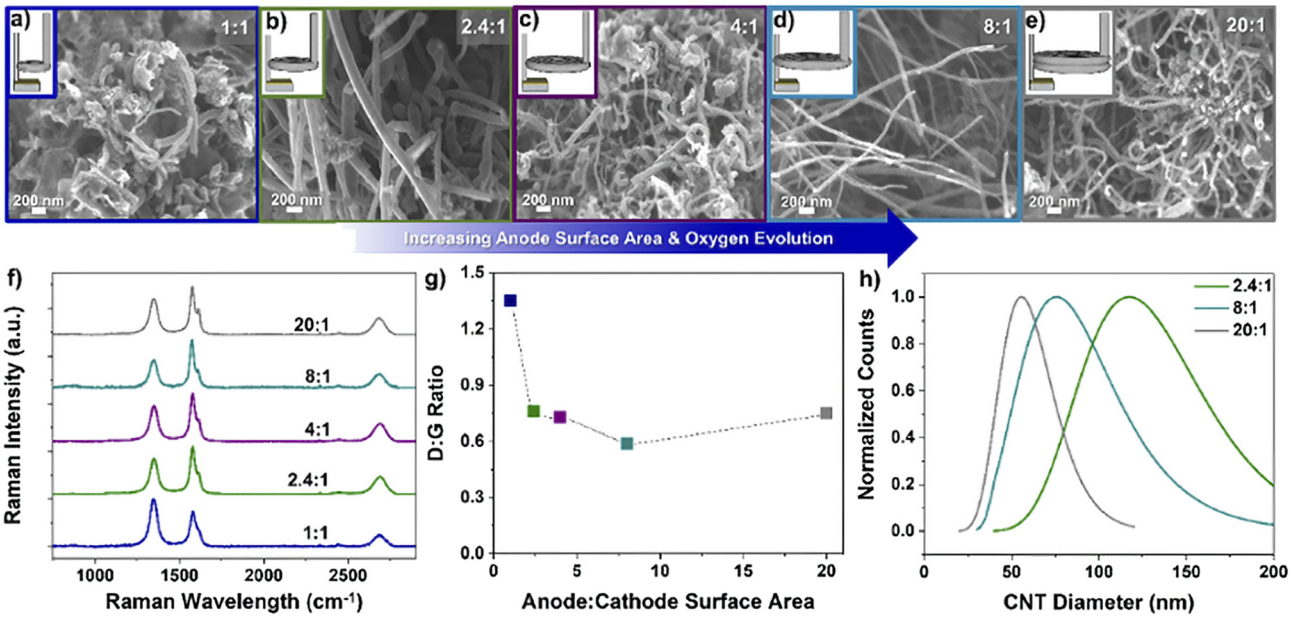

Fig. 12 Different anode to cathode surface area ratios (A : C) and the resulting carbon product using a Ni/Al_2O_3 anode with 5 nm Fe on stainless steel cathode; a) 1 : 1, b) 2.4 : 1, c) 4 : 1, d) 8 : 1, e) 20 : 1 and f) Raman spectra, g) D : G ratio, and h) CNT diameter distribution at ratios of 2.4 : 1, 8 : 1, and 20 : 1.[66]

In some cases, a solid electrolyte is utilized as an anode to act as an oxygen ion conductor. ZrO_2 was expected to fasten oxygen evolution.[67] The anode contains a ZrO_2 tube filled with carbon power to enhance electrical conductivity, and a stain steel pipe inserts in the carbon power and connects to a power supply.[67] However, the experimental results were far from satisfying. The conductive carbon diffused in the ZrO_2 lattice and reacted with oxygen to reproduce CO_2.[67] Thus, the reason for unsatisfying CO_2 conversion could be the technical design of the anode.

It Is also worth mentioning that simply increasing the anode surface largely helped the oxygen ion mass transfer, reduced oxide build-up on the cathode surface, and controlled CNTs size, as shown in Fig. 12.[66] Notably, the ratio of 20 : 1 was not favoured for CNTs growth, which can be explained by the dramatic area difference between the electrodes. The noteworthy difference resulted in a mismatched electric field, leading to low current efficiency.

2.4 Temperature

Temperature plays a critical role in electrolytic processes, product compositions, and material structures of produced carbon. For example, CNTs are more likely to form at operation temperatures lower than 700 °C, while CNS or CO favours higher temperatures.[53] Fig. 5 describes how temperatures and voltages affect the reactions.[74] Under the same potential, different reactions are thermodynamically favourable at different temperatures.

Temperature easily changes electrolyte properties, which later affects CO_2 absorption and conversion. Increasing temperature leads to a reduction in the stability of carbonates and CO_2 solubility.[67] Increasing temperatures shift the decomposition equilibrium towards the product side, producing more metal oxides and CO_2. The CO_2 volumetric mass transfer coefficients in carbonates decreased with increasing temperature, which negatively influences CO_2 physical dissolution.[89] CO_2 chemical dissolution, specifically the formation of CO_3^{2-} in eqn (3), is also weakened with increasing temperatures. For carbonates, it is even worse as heat decomposition results in related instability and then decreases CO_2 solubility with increasing temperatures.[67] In addition, the diffusion rate of carbonate ions directly corresponded to temperatures, which obeyed Arrhenius' Law.[107] An experimental data sample is shown in Table 5. Based on the data and Arrhenius' Law, the activation energy is calculated to be 35.8 kJ mol^{-1}. It is also revealed that temperature effects on CO_3^{2-} diffusion are relatively small.

The increased temperature can bring some negative effects to the electrolysis. The electrical resistance of electrolytes typically decreases as temperature increases.[71] For example, the current increased by 500 mA from 550 °C to 650 °C, and carbon layers were produced faster and thicker as the kinetics and diffusion rate increased.[71] Other

Table 5 Evolution of the diffusion coefficient with temperature in LiF–NaF–Li_2CO_3 (ref. 107)

Temperature (K)	$D \times 10^5$ (cm^2 s^{-1})
973	4.46
993	4.82
1023	5.31
1043	5.90
1063	6.54

Table 6 Estimated carbon deposition rates and current efficiencies during electrolysis in molten Li_2CO_3–K_2CO_3 at various temperatures and voltages[73]

Voltage (V)	Temperature (°C)	Time (h)	Deposition rate (g cm^{-2} h^{-1})	Current efficiency (%)
3	540	1.0	0.0306	91
3	593	1.0	0.0306	92
3	700	1.0	0.0613	90
4	540	1.0	0.0917	99
4	593	1.0	0.0851	100
4	700	1.0	0.0488	85
5	540	1.0	0.0712	98
5	593	1.0	0.0665	88
5	700	1.0	0.0248	65
5	540	0.5	0.1107	78
5	593	0.5	0.0874	89
5	700	0.5	0.0400	73

researchers pointed out that lower salt resistance did not necessarily mean higher current efficiency (Table 6).[73] The maximum current efficiency remains stable under varying temperatures but varies at different voltages. Thus, the optimal operation conditions require further investigation to determine.

Monitoring temperature can help achieve the desired structure and composition of carbon products. With the same operating conditions except for temperatures, a honeycomb structure of carbon was observed at 577 °C, but nanotubular carbon was obtained at an elevated temperature above 600 °C.[91] Another similar case was the carbon nanostructures changed under 2.6 V, and temperature varied from 650 °C to 850 °C.[100] At 650 °C, the produced carbon was thick graphite. With the temperature increasing to 750 °C, flat graphite sheets with graphene were observed. A further increase in temperature to 850 °C resulted in flatter sheets of graphene with fewer layers.[100] An increasing temperature also encourages the development of CNTs and suppresses the growth of CNS when transition metals, such as Ni, Cr, and Fe, are used as catalysts.[53] As shown in Table 7, combustion activation energy decreased with increasing operation temperature under the same voltage supply. As the energy barrier decreases with higher temperature, it is easier for carbon to deposit on the cathode, which matches the increased deposition rate in Table 6. This lower energy barrier could also explain why smaller carbon particle sizes were obtained.[73] From Table 8, it is seen that

Table 7 Average values of combustion activation energy for carbon samples deposited in Li_2CO_3–K_2CO_3 at various temperatures and voltages[73]

Temperature (°C)	Cell voltage		
	3.0 V	4.0 V	5.0 V
	E_a (kJ mol^{-1})		
540	158	165	171
593	152	158	160
700	131	142	148

Table 8 Elemental composition of carbon deposited after 1 h electrolysis in Li_2CO_3–K_2CO_3 at (a) 593 °C and different cell voltages, and (b) 4.0 V and different molten salt temperatures[73]

Element	Weight%		
(a) Cell voltage	3.0 V	4.0 V	5.0 V
C (K)	83.39	85.20	88.54
O (K)	12.80	13.85	10.71
K (K)	0.55	0.28	0.45
Cr (K)	1.20	—	—
Fe (K)	2.07	0.68	0.47
(b) Temperature (°C)	540	593	700
C (K)	83.56	85.20	92.33
O (K)	13.46	13.85	5.65
K (K)	1.12	0.28	1.73
Cr (K)	0.79	—	—
Fe (K)	1.83	0.68	0.28

increasing operating temperatures resulted in higher carbon contents and lower O, Fe, and K contents, except for Cr. Higher voltage and temperature surprisingly had a passivation effect on the anode, reducing Cr and Fe contents in the carbon.[73]

Not only the electrolysis temperature but the drying temperature following the washing could change the composition of the products. Washed carbon samples were dried at 80, 400, and 1000 °C, and it is reported that carbon nanoparticles at 400 °C contained the highest surface area detected by BET and the largest Li and Na capacity amounts, providing superior electrochemical performances.[70] It is also found that the in-plane layer stacking dimension decreases gradually from 74 nm at 80 °C to 29 nm at 1000 °C.[70]

2.5 Voltage & energy efficiency

The voltage of the system has an impact on the contents and the morphology of the products. As shown in Fig. 5, voltage is as important as temperature, and both play a significant role in determining the electrolysis reaction. However, a higher voltage supply also indicates large energy consumption. Considering the energy costs, the balance of product quality and operation settings needs to be carefully maintained to achieve the optimum profit. Additionally, the voltage should be carefully balanced: sufficient current enlarges carbon deposition rate while higher current results in a strong electric field and leads to difficult carbonate anion diffusion towards the cathode; Table 6 shows a decrease in deposition rate when the voltage increased from 4 to 5 V at 540 °C. The behaviour can be explained by the formation of CO, but the influence of the electric field on the diffusion of carbonate ions has not been investigated.

The electrolysis voltage should vary depending on the electrolyte cations and the amount of energy needed to split carbonates at a particular temperature. To minimize impurities in carbon products, the voltage, in general, should be less than the theoretical deposition potential of alkali cations or chloride evolution of electrolytes. Taking Li_2CO_3 electrolyte as an example, the applied voltage should be

controlled between −2.964 and −1.719 V at 600 °C to produce carbon and avoid Li formation using data from Table 4. However, this range is not mandatory in practice, which means the voltage setting can exceed the potential of alkali metal formation. Numerous research studies were conducted under much higher voltage. It is believed that, under an operating voltage higher than alkali deposition potential, the deposited alkali metal particles can act as nucleation sites and encourage the growth of unique nanostructures. Ge, Ni, Fe, and other metals were observed in SEM or TEM to grow CNTs by serving as two ends of the tube structure.[44,95]

Similar to how they can be modified by temperature, the compositions and architectures of the products can also be altered by voltage. It is common knowledge that at a current between 0–2 A cm^2, CO_2 converts into carbon, and no gas is generated at the cathode, while a higher current can lead to the formation of CO gas.[108] With the extremely large current of 33 A, nano-diamonds could be produced at low pressure at 800 °C.[109] At 2.8 V, the carbon product appears to be a carbon film. When the voltage increases to 4.0 V, the carbon presents a flocculent exterior.[35] Carbon, as well as alkaline metal depositions, decide the final nanostructures of formed carbon, especially at a high cell voltage (over 5 V).[71] The SEM images of the carbon obtained at different voltages are shown in Fig. 14. As shown in Table 9, the specific surface area of carbon increases with increasing voltages. Similar results are also observed in Ijije's article.[73] The particle sizes of carbon become smaller with rising current densities.[91] However, the crystallinity of carbon does not change with voltage. Kaplan and his colleagues operated the experiments under −1.6, −2.4, and −6.0 V remaining other parameters the same.[108] From Kaplan's data, the crystallinity of carbon products was similar but slightly reduced when the voltage became more negative. Along with more negative voltage, the side reactions play a more important role. The carbon samples grow more impurities, including oxygen and lithium.[108] The weight percentage changes aligned with the theories of alkali metal deposition are expressed in eqn (6). Mesopores increase with elevated voltage.[73] Additionally, a combination of high and low current densities in the process can lead to different carbon nanostructures. For instance, amorphous carbon is obtained if the current density is kept at 100 mA cm^{-2} for the cathode throughout the process. While CNF is formed when the current density is set low initially, *e.g.*, 5 mA cm^{-2} for 1 h, and gradually increases to 100 mA cm^{-2} and remains at this density.[92] Ren *et al.* suggested the difference in carbon nanostructure is caused by the anode metal deposition at low current density, such as Ni, which is critical for CNF nucleation formation.[92]

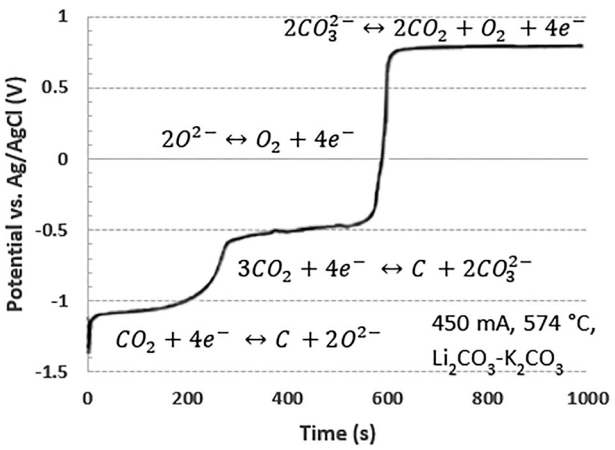

Fig. 13 Chrono-potentiometric plots for anodic oxidation of the electro-deposited carbon in Li_2CO_3–K_2CO_3 at 574 °C, reproduced from ref. 41 with open-access permission from the Royal Society of Chemistry, copyright 2014.

The activity of oxygen ions is also affected by voltages. Fig. 13 shows the Chrono-potentiometric plots for the anodic oxidation of carbon. The rapid increase in the current between the second and third plateaus demonstrates the activity of oxygen ions in the molten salt is slower than the activity of CO_3^{2-}. The CVs Ijije and his team obtained show there was no clear signal of anodic discharge of the O^{2-} ions, which also indicates the amount of O^{2-} ions generating O_2 is less than the amount of O^{2-} ions produced by carbonate ion splitting.[41] The loss of oxygen ions can be explained by eqn (3), where the O^{2-} ions absorb carbon dioxide and form carbonate ions. However, how different voltages influence the O^{2-} transfer and oxygen generation has not been fully reported yet.

The required voltage is directly associated with current efficiency and energy consumption. Although high voltage may result in a desirable morphology of carbon product, the energy penalty might overweight the improvement. Fig. 15 shows the highest temperature or voltage is not the optimal condition for reaction efficiency or energy consumption. Temperature and voltage should be selected for best efficiency, preferred carbon structure, and affordable energy consumption. Harsh operation conditions are always accompanied by excessive energy consumption. Tang's research results demonstrate the lowest energy consumption was around 38 kW h kg^{-1} CO_2 at 3 V and 550 °C, which aligned with Yin's finding.[35,71] It should be emphasised that their calculations of energy consumption did not account for the heat needed to maintain high temperatures. Lack of heat consumption could result in mistakes when determining the best operating conditions because temperatures and voltages both affect how quickly carbon is deposited. Most importantly, more research should be conducted in the future to determine how voltage affects carbon deposition rate and its nanostructures.

2.6 Composition of inlet gas

Power plant flue gas usually contains various gas components, and their compositions are changed with combustion conditions.[110,111] CO_2, O_2, SO_2, NO_x, and vapour are commonly identified in the flue gas. Molten salt electrolysis has been performed under various CO_2

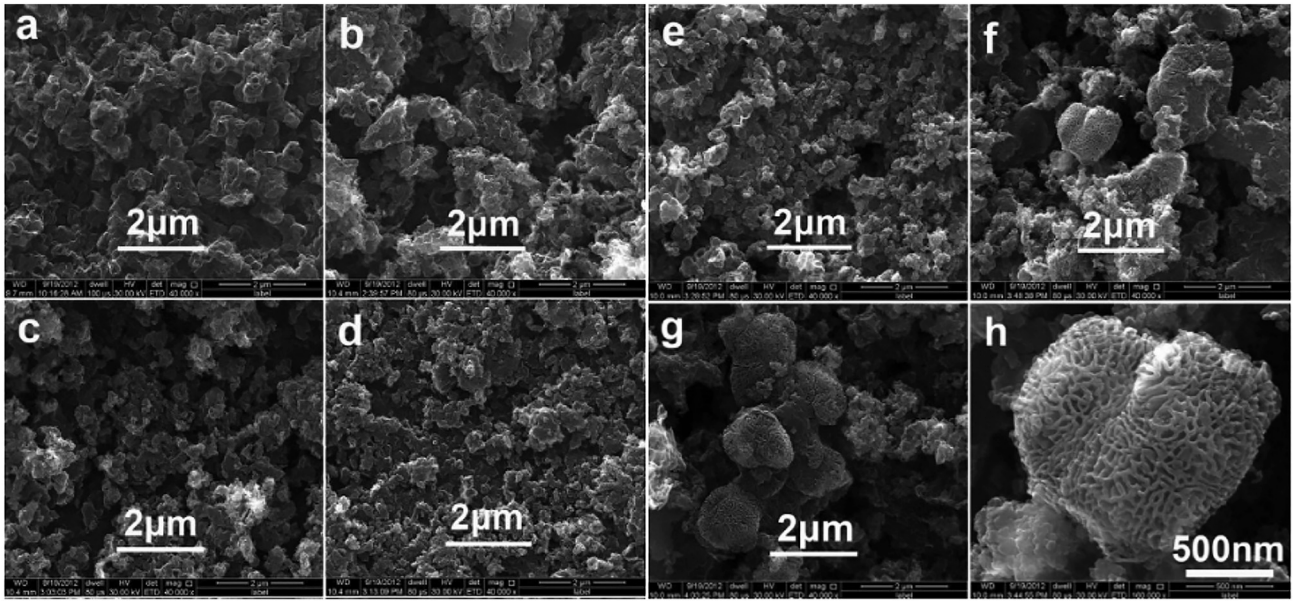

Fig. 14 SEM images of carbon powders obtained under cell voltages of 3.0 V (a), 3.5 V (b), 4.0 V (c), 4.5 V (d), 5.0 V (e), 5.5 V (f), (h) and 6.0 V (g) at 450 ° C in Li_2CO_3–Na_2CO_3–K_2CO_3 mixture.[71]

concentrations, ranging from 0.04% (atmospheric concentration), 14% (typical CO_2 concentration in the flue gas), to 100%.[35,57,92] It is unnecessary to concentrate CO_2 prior to electrolysis. It was reported that half of the CO_2 can be absorbed from gas with 14% CO_2 and converted into carbon with 90% current efficiency.[57] Even for 0.04% carbon dioxide concentration, the centration step is not required, and current efficiency can still be near 100%.[92]

However, other gas impurities' effects have not been fully reported. Investigating how these impurities affect the electrolysis reaction and products is required before applying this electrolysis approach to commercial post-combustion plants. N_2, as an inert gas, is often used as the carrier gas for flow rate and pressure modifications. However, O_2-related effects have not yet been fully observed. The influence of vapour was carried out using LiOH additives as an alternative because of the difficulty in the quantification of vapour added to the system.[48] Under a typical operating condition of molten salt electrolysis, vapour has a good chance of undergoing the water-splitting reaction, which expects to have a significant impact on the electrolytic process.[47,48,112] Shown in Table 10, H_2 is the major product, over 50% in all cases, when CO_2 is fed into molten carbonates with LiOH additives. With appropriate conditions, the current efficiency for syngas could achieve 90%.[112] Ji's report shows similar results that an increase of 0.5 V significantly promoted CO formation and resulted in 33.6% CO and 64.2% H_2 in the gas products.[48]

SO_2 in the flue gas undergoes electrolysis in the molten carbonate salt with Li_2SO_4 additive. Similar to CO_2, SO_2 can react with O^{2-} and form Li_2SO_4, which is later reduced into sulfides or sulphur. The resulting sulphur is inserted into deposited carbon nanostructures, forming sulphur-doped carbon.[79] Instead of accumulating in molten salts, it is observed that sulphur element was found at the gas outlet of the cathode.[113] Sulphur contents in the system can also react with carbon to form CS_2, which is helpful in removing imperfect carbon and leads to graphitization over 500 °C. It suggests that the deposited S and S^{2-} also contribute to the low-temperature graphitization.[114] In the end, sulphur contents in the feed stream can be completely captured.[34]

Eqn (14) and (15) are the two possible reactions happening in Li carbonate molten salts.[113] Li_2SO_4 has lower decomposition potentials compared to Li_2CO_3, so the sulphur reduction current is limited by diffusion.[113] CO_2 can still be converted into carbon or CO, but with reduced efficiency; for example, the CO production faradaic efficiency with SO_2 inlet is reduced to 54%, as shown.[113]

$$4Li_2CO_3 + 4SO_2 \rightarrow Li_2SO_4 + Li_2S + 4CO_2 \quad (14)$$

Table 9 BET surface area ($m^2\ g^{-1}$) of the carbon powders prepared under different conditions[71]

	3.5 V	3.0 V	4.0 V	4.5 V	5.0 V	5.5 V	6.0 V
450 °C	306.76	558.10	536.41	613.76	526.60	868.31	856.26
550 °C	—	—	—	212.39	—	—	—
650 °C	—	—	—	101.89	—	—	—

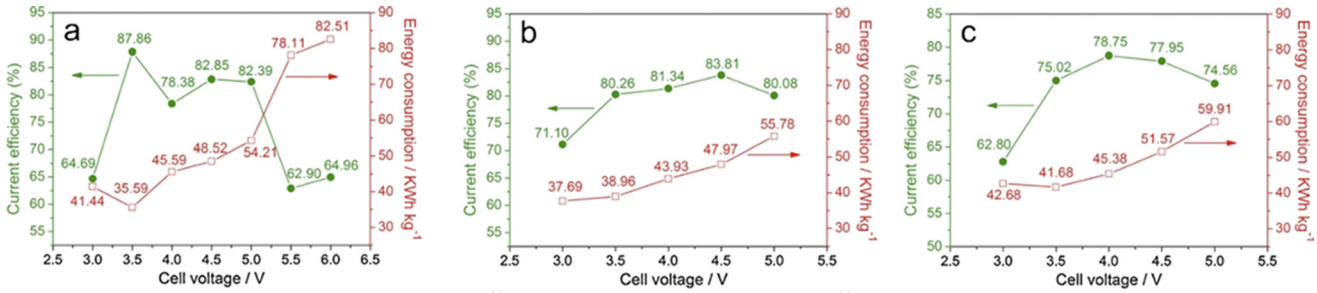

Fig. 15 Energy consumption and current efficiency under different cell voltages at 450 °C (a), 550 °C (b), and 650 °C (c).[71]

$$4Li_2O + 4SO_2 \rightarrow 3Li_2SO_4 + Li_2S \quad (15)$$

The Gibbs free energies show both reactions are thermodynamically feasible, but the SO_2 absorption rate of melts is slower than the reaction.[113] If oxygen is also fed into the system and the volume ratio of SO_2 to O_2 is less than 2, SO_2 can be consumed rapidly through the following reactions shown in eqn (16) and (17).[113]

$$2Li_2CO_3 + 2SO_2 + O_2 \rightarrow 2Li_2SO_4 + 2CO_2 \quad (16)$$

$$2Li_2O + 2SO_2 + O_2 \rightarrow 2Li_2SO_4 \quad (17)$$

Inlet gas flow rate and CO_2 concentration are additional parameters that can be tuned to suit CO formation. As shown in Fig. 16(a), the conversion of CO_2 to CO increases with rising flow rates, but the increase reaches a plateau at a certain flow rate. The high gas flow rate improves the mixing of gas and molten salts and the dispersion of ions.[42] But due to the low residence time of CO_2, complete carbon deposition cannot be reached, and the formation of CO is favoured in this case. However, CO formation can be suppressed by further increasing gas flow rates. Overall, a 2-electron cathodic reaction is favoured in this case to form CO gas.[42] Fig. 16(b) provides the ratio of CO_2 concentration to its CO product. When CO_2 concentration increased from 5% to 15%, CO concentration correspondingly jumped from 0 to 90%.

Table 10 Gaseous products detected at the exit of a molten salt cell with $Li_{1.43}Na_{0.2}$ $K_{0.2}$ CO_3 salt and 10 wt% LiOH additive[48]

	Electrolysis parameters		Gas content		
No.	Temperature (°C)	Voltage (V)	CH_4 (%)	CO (%)	H_2 (%)
1	450	2.0	18.2	—	81.7
2	500	2.0	22.1	—	88.6
3	550	2.0	40.1	—	59.5
4	600	2.0	30.4	0.1	69.3
5	650	2.0	27.3	2.4	69.9
6	550	1.0	—	—	100
7	550	1.5	—	—	100
8	550	2.5	13.3	9.2	77.2
9	550	3.0	5.4	20.2	74.0
10	550	3.5	1.9	33.6	64.2

3 Conclusion & future challenges

Molten salt CO_2 electrolysis is an innovative CO_2 capture and conversion method targeting power plant flue gas to achieve CO_2 zero emission. This molten salt system presents multiple advantages, including high current efficiency, simper solid separation of produced carbon, engineered carbon nanostructures, and positive cash flow. Carbonates hold better CO_2 absorption ability and higher current efficiency compared to chlorides as electrolytes. Considering metal deposition side reactions and melting points, lithium, sodium, and potassium carbonates are widely used and combined. Oxide additives are favoured to increase gas sorption, especially in chlorides, and also impact carbon nanostructures. The cathode is another factor influencing carbon nanostructures, and popular choices are Fe, Ni, Pt, their metal oxides, and alloys. Anode is responsible for the critical oxygen evolution so the materials should have a strong durability and anti-corrosion ability, such as metal oxides and alloys. Temperature and voltages are the two significant parameters in this electrolysis, as they control the activation energy of the electrolysis. Higher temperature suppresses carbon formation but improves CO production. The study of voltage focuses on not only the electrolysis potentials but also the energy consumption for optimal efficiency.

However, molten salt CO_2 electrolysis leaves some research gaps. The first challenge is scaling up and corrosion's effects on the equipment. To date, all the research results are produced from a lab-scaled system, and there has not been a commercial-scaled system yet. The mass and energy balance, energy efficiency, cost of materials, the activity of electrocatalysts, waste heat utilization, and system designs are unknown or obscure engineering aspects.[74] There exist obstacles in maintaining a continuous operation, recovering salts, and removing carbon that has grown on the cathode. Although Licht's research team did suggest a method for separating salt electrolytes, some problems still appear to prevent the commercialization of electrolysis. These problems include the energy loss associated with preheating the separation device to 750 °C, carbon build-up on the cathode surface, and potential device corrosion.[45] For the recovery process and saving acid from dissolving carbonates in current lab-

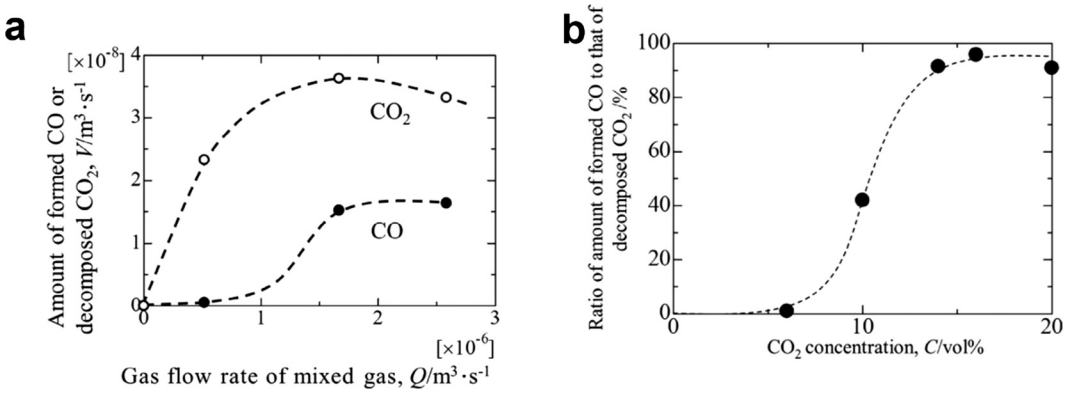

Fig. 16 (a) Amounts of decomposed CO_2 gas and produced CO gas as a function of inlet gas flow rate; (b) ratio of the amount of formed CO gas to that of decomposed CO_2 gas as a function of the initial gas concentration of CO_2.[42]

scale experiments, a molten $CaCl_2$ dissolver was proposed to extract carbon from CaO and $CaCO_3$, which are insoluble in water.[115] But the corrosion tests of this method should be obtained to compare the influence of $CaCl_2$ and other soluble carbonates. Furthermore, equipment and electrodes can corrode rapidly due to high temperatures and the corrosive nature of molten salts under general electrolysis operations. More research is therefore needed to develop reliable electrodes that are more affordable, perform better, and balance absorption kinetics and reaction mechanisms. To enhance CO_2 conversion efficiency, the shape and surface area of electrodes should be investigated.

The formation of uniform carbon nanostructures can be another challenge. Morphology of carbon products is sensitive to operating conditions; for example, MWCNTs took up 40 vol% of Novoselova's cathode sample and about 80% CNFs in Ren's results.[81,98] In the latest report, the highest percentage of a specific nanostructure was 98%.[44] A 100% uniform carbon nanostructure has not been obtained. In addition to the carbon nanostructure, it is important to investigate the carbon deposition rate with different additives. Furthermore, these reports made no comment on the factors that affect the rate of carbon deposition or the effectiveness of CO_2 capture; hence, further research is necessary to close this knowledge gap.

More fundamental research is required to fully understand the electrolysis reaction mechanisms, such as quantifying oxides and carbonate ion concentration changes and their mass transfer. Although the operating parameters and their effects on electrolysis performances and products have been investigated, there are still some challenges, such as quantifying rate-determining step and monitoring oxygen ion mass transfer during electrolysis and CO_2 absorption. The influences of the electric field on carbonate anions should also be examined to study the diffusion mechanism of carbonate anions towards the cathode. The density functional theory (DFT) has been employed to interpret the fundamentals of metal particles as nucleation sites for the formation of nano carbon products.[97] Experimental validations are essentially expected. More DFT research and calculation should be performed to provide a more comprehensive study of different parameters and conditions at the molecular level. There also lacks records for a full analysis of the effects of flue gas impurities, especially for NO_x, water vapour, and oxygen. Besides its compositions, the conditions of the flue gas, including pressure and temperature, have not been well studied. Other fundamental knowledge deserves attention, including electrode/electrolyte interface analysis, mass transfer between gaseous CO_2, liquid electrolytes, and solid electrodes, reactors' influences on electrolysis, CO_2/electrolyte fluid dynamics, and more. Other basic analysis, such as safety and economy analysis, is also missing in this field.

Conflicts of interest

The authors declare no conflict of interest.

Acknowledgements

The authors would like to acknowledge the financial support received from Natural Resources Canada (NRCan) CCUS program and Western University Ontario.

References

1 R. A. Smith, *Air and rain: the beginnings of a chemical climatology*, Longmans Green and Co., London, 1872.
2 G. Nonhebel, A commercial plant for removal of smoke and oxides of sulphur from flue gases, *Trans. Faraday Soc.*, 1936, **32**, 1291–1296.
3 OECD, *20 Years of Carbon Capture and Storage: Accelerating Future Deployment | OECD iLibrary*, [cited 2023 May 8], Available from: **https://www.oecd-ilibrary.org/energy/20-years-of-carbon-capture-and-storage_9789264267800-en**.
4 H. Herzog, *An Introduction to CO2 Separation and Capture Technologies*, MIT Energy Laboratory, 1999, pp. 1–8, [cited 2023 May 8], Available from: **https://sequestration.mit.edu/pdf/introduction_to_capture.pdf**.

5 OECD/IEA, *Prospects for CO2 Capture and Storage – Analysis*, IEA, [cited 2023 May 8], Available from: **https://www.iea.org/reports/prospects-for-co2-capture-and-storage**.
6 J. Farrell, Carbon Capture – CCS: how regulatory, technological, and legislative failures have dogged the carbon mitigation strategy throughout the decades, *Journal of Science Policy & Governance*, 2018, **12**(1), 1–22.
7 A. Midttun, The Negotiated Political Economy of a Heavy Industrial Sector: The Norwegian Hydropower Complex in the 1970s and 1980s, *Scan. Polit. Stud.*, 1988, **11**(2), 115–144.
8 J. Zillman, *A History of Climate Activities*, 2015, [cited 2022 Oct 18], Available from: **https://public.wmo.int/en/bulletin/history-climate-activities**.
9 H. Ritchie and M. Roser, *CO_2 and Greenhouse Gas Emissions*, Our World in Data, 2020, [cited 2022 Sep 19], Available from: **https://ourworldindata.org/emissions-by-sector**.
10 IEA, *Global Energy Review: CO2 Emissions in 2021*, IEA, 2021, [cited 2022 Oct 18], Available from: **https://iea.blob.core.windows.net/assets/c3086240-732b-4f6a-89d7-db01be018f5e/GlobalEnergyReviewCO2Emissionsin2021.pdf**.
11 R. Shirmohammadi, A. Aslani, R. Ghasempour and L. M. Romeo, CO2 utilization via integration of an industrial post-combustion capture process with a urea plant: Process modelling and sensitivity analysis, *Processes*, 2020, **8**(9), 1144.
12 D. Kearns, H. Liu and C. Consoli, *Technology readiness and costs of CCS*, 2021, [cited 2022 Oct 18], Available from: **https://www.globalccsinstitute.com/wp-content/uploads/2021/04/CCS-Tech-and-Costs.pdf**.
13 SCCS, *Sleipner Details*, [cited 2022 Sep 26], Available from: **https://www.geos.ed.ac.uk/sccs/project-info/2**.
14 SaskPower, *Carbon Storage Research Centre*, SaskPower, [cited 2022 Oct 18], Available from: **https://www.saskpower.com/our-power-future/infrastructure-projects/carbon-capture-and-storage/carbon-storage-research-centre**.
15 Alberta Government, *Quest Carbon Capture and Storage project: annual report, 2020 - Open Government*, 2020, [cited 2022 Jul 16], Available from: **https://open.alberta.ca/publications/quest-carbon-capture-and-storage-project-annual-report-2020**.
16 Province of British Columbia, *British Columbia's Carbon Tax*, Province of British Columbia, [cited 2023 Feb 28], Available from: **https://www2.gov.bc.ca/gov/content/environment/climate-change/clean-economy/carbon-tax**.
17 F. Qin, S. Wang, A. Hartono, H. F. Svendsen and C. Chen, Kinetics of CO2 absorption in aqueous ammonia solution, *Int. J. Greenhouse Gas Control*, 2010, **4**(5), 729–738.
18 H. Yamada, Amine-based capture of CO2 for utilization and storage, *Polym. J.*, 2021, **53**(1), 93–102.
19 A. Reyes-Lúa, K. Jordal and SINTEF Energy Research, *Current and emerging industrial-scale CO_2 capture, A brief overview, TG2 Briefing Report on Industrial CO_2 capture-CCUS Projects Network Thematic Reports*, 2019, pp. 1–33.
20 G. Puxty, R. Rowland, A. Allport, Q. Yang, M. Bown and R. Burns, *et al.*, Carbon dioxide postcombustion capture: A novel screening study of the carbon dioxide absorption performance of 76 amines, *Environ. Sci. Technol.*, 2009, **43**(16), 6427–6433.
21 S. Y. Lee and S. J. Park, A review on solid adsorbents for carbon dioxide capture, *J. Ind. Eng. Chem.*, 2015, **23**, 1–11.
22 NRG Energy Inc., *Petra Nova*. NRG Energy, [cited 2022 Dec 19], Available from: **https://www.nrg.com/case-studies/petra-nova.html**.
23 J. Artz, T. E. Müller, K. Thenert, J. Kleinekorte, R. Meys and A. Sternberg, *et al.*, Sustainable Conversion of Carbon Dioxide: An Integrated Review of Catalysis and Life Cycle Assessment, *Chem. Rev.*, 2018, **118**(2), 434–504.
24 H. Zeng, X. Qu, D. Xu and Y. Luo, Porous Adsorption Materials for Carbon Dioxide Capture in Industrial Flue Gas, *Front. Chem.*, 2022, **10**, 1–18, Available from: **https://www.frontiersin.org/articles/10.3389/fchem.2022.939701**.
25 D. Aaron and C. Tsouris, Separation of CO2 from flue gas: A review, *Sep. Sci. Technol.*, 2005, **40**(1–3), 321–348.
26 C. H. Yu, C. H. Huang and C. S. Tan, A review of CO2 capture by absorption and adsorption, *Aerosol Air Qual. Res.*, 2012, **12**(5), 745–769.
27 S. Overa, B. H. Ko, Y. Zhao and F. Jiao, Electrochemical Approaches for CO2 Conversion to Chemicals: A Journey toward Practical Applications, *Acc. Chem. Res.*, 2022, **55**(5), 638–648.
28 S. Simon Araya, V. Liso, X. Cui, N. Li, J. Zhu and S. L. Sahlin, *et al.*, A Review of The Methanol Economy: The Fuel Cell Route, *Energies*, 2020, **13**(3), 596.
29 S. Kar, A. Goeppert and G. K. S. Prakash, Integrated CO2 Capture and Conversion to Formate and Methanol: Connecting Two Threads, *Acc. Chem. Res.*, 2019, **52**(10), 2892–2903.
30 Z. Z. Yang, L. N. He, Y. N. Zhao, B. Li and B. Yu, CO2 capture and activation by superbase/polyethylene glycol and its subsequent conversion, *Energy Environ. Sci.*, 2011, **4**(10), 3971–3975.
31 T. A. Atsbha, T. Yoon, P. Seongho and C. J. Lee, A review on the catalytic conversion of CO2 using H2 for synthesis of CO, methanol, and hydrocarbons, *J. CO_2 Util.*, 2021, **44**, 101413.
32 L. Cui, C. Liu, B. Yao, P. P. Edwards, T. Xiao and F. Cao, A review of catalytic hydrogenation of carbon dioxide: From waste to hydrocarbons, *Front. Chem.*, 2022, **10**, 1–25, Available from: **https://www.frontiersin.org/articles/10.3389/fchem.2022.1037997**.
33 H. S. Shafaat and J. Y. Yang, Uniting biological and chemical strategies for selective CO2 reduction, *Nat. Catal.*, 2021, **4**(11), 928–933.
34 R. Pachaiappan, S. Rajendran, P. Senthil Kumar, D.-V. N. Vo and T. K. A. Hoang, A review of recent progress on photocatalytic carbon dioxide reduction into sustainable energy products using carbon nitride, *Chem. Eng. Res. Des.*, 2022, **177**, 304–320.
35 H. Yin, X. Mao, D. Tang, W. Xiao, L. Xing and H. Zhu, *et al.*, Capture and electrochemical conversion of CO2 to

value-added carbon and oxygen by molten salt electrolysis, *Energy Environ. Sci.*, 2013, **6**(6), 1538–1545.
36 E. S. Rubin, J. E. Davison and H. J. Herzog, The cost of CO2 capture and storage, *Int. J. Greenhouse Gas Control*, 2015, **40**, 378–400.
37 S. Licht, Co-production of cement and carbon nanotubes with a carbon negative footprint, *J. CO2 Util.*, 2017, **18**, 378–389.
38 V. Khanna, B. R. Bakshi and L. J. Lee, Carbon Nanofiber Production, *J. Ind. Ecol.*, 2008, **12**(3), 394–410.
39 H. Y. Teah, T. Sato, K. Namiki, M. Asaka, K. Feng and S. Noda, Life Cycle Greenhouse Gas Emissions of Long and Pure Carbon Nanotubes Synthesized via On-Substrate and Fluidized-Bed Chemical Vapor Deposition, *ACS Sustainable Chem. Eng.*, 2020, **8**(4), 1730–1740.
40 V. Kaplan, E. Wachtel and I. Lubomirsky, CO2 to CO Electrochemical Conversion in Molten Li2CO3 Is Stable with Respect to Sulfur Contamination, *J. Electrochem. Soc.*, 2013, **161**(1), F54.
41 H. V. Ijije, R. C. Lawrence, N. J. Siambun, S. M. Jeong, D. A. Jewell and D. Hu, *et al.*, Electro-deposition and re-oxidation of carbon in carbonate-containing molten salts, *Faraday Discuss.*, 2014, **172**, 105–116.
42 F. Matsuura, T. Wakamatsu, S. Natsui, T. Kikuchi and R. O. Suzuki, CO gas production by molten salt electrolysis from CO2 gas, *ISIJ Int.*, 2015, **55**(2), 404–408.
43 X. Liu, X. Wang, G. Licht and S. Licht, Transformation of the greenhouse gas carbon dioxide to graphene, *J. CO2 Util.*, 2020, **36**, 288–294.
44 X. Liu, G. Licht, X. Wang and S. Licht, Controlled Transition Metal Nucleated Growth of Carbon Nanotubes by Molten Electrolysis of CO2, *Catalysts*, 2022, **12**(2), 137.
45 X. Wang, G. Licht and S. Licht, Green and scalable separation and purification of carbon materials in molten salt by efficient high-temperature press filtration, *Sep. Purif. Technol.*, 2021, **255**, 117719, Available from: **https://journals.scholarsportal.info/details/13835866/v255icomplete/nfp_gassapsbehpf.xml**.
46 E. Laasonen, V. Ruuskanen, M. Niemelä, T. Koiranen and J. Ahola, Insights into carbon production by CO2 reduction in molten salt electrolysis in coaxial-type reactor, *J. Environ. Chem. Eng.*, 2022, **10**(1), 106933.
47 O. Al-Juboori, F. Sher, U. Khalid, M. B. K. Niazi and G. Z. Chen, Electrochemical Production of Sustainable Hydrocarbon Fuels from CO2Co-electrolysis in Eutectic Molten Melts, *ACS Sustainable Chem. Eng.*, 2020, **8**(34), 12877–12890.
48 D. Ji, Q. Jia, C. Zhu, W. Dong, H. Wu and G. Wang, A New, Efficient Conversion Technology to Transform Ambient CO2 to Valuable, Carbon-Based Fuel via Molten Salt Electrochemistry, *Appl. Sci.*, 2022, **12**(17), 8874.
49 S. Arcaro, F. A. Berutti, A. K. Alves and C. P. Bergmann, MWCNTs produced by electrolysis of molten carbonate: Characteristics of the cathodic products grown on galvanized steel and nickel chrome electrodes, *Appl. Surf. Sci.*, 2019, **466**, 367–374.
50 X. Chen, H. Zhao, H. Xie, J. Qu, X. Ding and Y. Geng, *et al.*, Tuning the preferentially electrochemical growth of carbon at the "gaseous CO2-liquid molten salt-solid electrode" three-phase interline, *Electrochim. Acta*, 2019, **324**, 134852.
51 X. Liu, J. Ren, G. Licht, X. Wang and S. Licht, Carbon Nano-Onions Made Directly from CO2 by Molten Electrolysis for Greenhouse Gas Mitigation, *Adv. Sustainable Syst.*, 2019, **3**(10), 1900056.
52 X. Wang, X. Liu, G. Licht and S. Licht, Calcium metaborate induced thin walled carbon nanotube syntheses from CO2 by molten carbonate electrolysis, *Sci. Rep.*, 2020, **10**(1), 1–7.
53 X. Wang, G. Licht, X. Liu and S. Licht, One pot facile transformation of CO2 to an unusual 3-D nano-scaffold morphology of carbon, *Sci. Rep.*, 2020, **10**(1), 1–12.
54 D. Tang, Y. Dou, H. Yin, X. Mao, W. Xiao and D. Wang, The capacitive performances of carbon obtained from the electrolysis of CO2 in molten carbonates: Effects of electrolysis voltage and temperature, *J. Energy Chem.*, 2020, **51**, 418–424.
55 X. Wang, F. Sharif, X. Liu, G. Licht, M. Lefler and S. Licht, Magnetic carbon nanotubes: Carbide nucleated electrochemical growth of ferromagnetic CNTs from CO2, *J. CO2 Util.*, 2020, **40**, 101218.
56 L. Hu, B. Deng, Z. Yang and D. Wang, Buffering electrolyte alkalinity for highly selective and energy-efficient transformation of CO2 to CO, *Electrochem. Commun.*, 2020, **121**, 106864.
57 L. Hu, B. Deng, K. Du, R. Jiang, Y. Dou and D. Wang, Tunable Selectivity and High Efficiency of CO2 Electroreduction via Borate-Enhanced Molten Salt Electrolysis, *iScience*, 2020, **23**(10), 101607.
58 R. Yu, B. Deng, K. Zheng, X. Wang, K. Du and D. Wang, A facile strategy to synthesize graphitic carbon-encapsulated core-shell nanocomposites derived from CO2 as functional materials, *Compos. Commun.*, 2020, **22**, 100464.
59 R. Yu, B. Deng, K. Du, D. Chen, M. Gao and D. Wang, Modulating carbon growth kinetics enables electrosynthesis of graphite derived from CO2 via a liquid–solid–solid process, *Carbon*, 2021, **184**, 426–436.
60 X. Chen, Z. Zhao, J. Qu, B. Zhang, X. Ding and Y. Geng, *et al.*, Electrolysis of Lithium-Free Molten Carbonates, *ACS Sustainable Chem. Eng.*, 2021, **9**(11), 4167–4174.
61 J. Yang, Y. Dou, H. Yang and D. Wang, A novel porous carbon derived from CO2 for high-efficient tetracycline adsorption: Behavior and mechanism, *Appl. Surf. Sci.*, 2021, **538**, 148110.
62 R. Jiang, M. Gao, X. Mao and D. Wang, Advancements and potentials of molten salt CO 2 capture and electrochemical transformation (MSCC-ET)process, *Curr. Opin. Electrochem.*, 2019, **17**, 38–46.
63 V. Kaplan, E. Wachtel, K. Gartsman, Y. Feldman and I. Lubomirsky, Conversion of CO[sub 2] to CO by Electrolysis of Molten Lithium Carbonate, *J. Electrochem. Soc.*, 2010, **157**(4), B552.
64 M. Gao, B. Deng, Z. Chen, M. Tao and D. Wang, Cathodic reaction kinetics for CO2 capture and utilization in molten

carbonates at mild temperatures, *Electrochem. Commun.*, 2018, **88**, 79–82.

65 M. Gao, B. Deng, Z. Chen, M. Tao and D. Wang, Enhanced kinetics of CO2 electro-reduction on a hollow gas bubbling electrode in molten ternary carbonates, *Electrochem. Commun.*, 2019, **100**, 81–84.

66 K. Moyer, M. Zohair, J. Eaves-Rathert, A. Douglas and C. L. Pint, Oxygen evolution activity limits the nucleation and catalytic growth of carbon nanotubes from carbon dioxide electrolysis via molten carbonates, *Carbon*, 2020, **165**, 90–99.

67 K. Otake, H. Kinoshita, T. Kikuchi and R. O. Suzuki, CO2 gas decomposition to carbon by electro-reduction in molten salts, *Electrochim. Acta*, 2013, **100**, 293–299.

68 W. Weng, L. Tang and W. Xiao, Capture and electro-splitting of CO2 in molten salts, *J. Energy Chem.*, 2019, 128–143.

69 S. Licht, B. Wang and H. Wu, STEP - A solar chemical process to end anthropogenic global warming. II: Experimental results, *J. Phys. Chem. C*, 2011, **115**(23), 11803–11821.

70 H. Groult, B. Kaplan, F. Lantelme, S. Komaba, N. Kumagai and H. Yashiro, *et al.*, Preparation of carbon nanoparticles from electrolysis of molten carbonates and use as anode materials in lithium-ion batteries, *Solid State Ionics*, 2006, **177**(9–10), 869–875.

71 D. Tang, H. Yin, X. Mao, W. Xiao and D. H. Wang, Effects of applied voltage and temperature on the electrochemical production of carbon powders from CO2 in molten salt with an inert anode, *Electrochim. Acta*, 2013, **114**, 567–573.

72 V. Kaplan, E. Wachtel, K. Gartsman, Y. Feldman and I. Lubomirsky, Conversion of CO2 to CO by Electrolysis of Molten Lithium Carbonate, *J. Electrochem. Soc.*, 2010, **157**(4), B552.

73 H. V. Ijije, C. Sun and G. Z. Chen, Indirect electrochemical reduction of carbon dioxide to carbon nanopowders in molten alkali carbonates: Process variables and product properties, *Carbon*, 2014, **73**, 163–174.

74 S. Licht, B. Wang, S. Ghosh, H. Ayub, D. Jiang and J. Ganley, A New Solar Carbon Capture Process: Solar Thermal Electrochemical Photo (STEP) Carbon Capture, *J. Phys. Chem. Lett.*, 2010, **1**(15), 2363–2368.

75 D. Pletcher, The cathodic reduction of carbon dioxide - What can it realistically achieve? A mini review, *Electrochem. Commun.*, 2015, **61**, 97–101.

76 B. Deng, Z. Chen, M. Gao, Y. Song, K. Zheng and J. Tang, *et al.*, Molten salt CO2 capture and electro-transformation (MSCC-ET) into capacitive carbon at medium temperature: Effect of the electrolyte composition, *Faraday Discuss.*, 2016, **190**, 241–258.

77 W. Xiao and D. Wang, The electrochemical reduction processes of solid compounds in high temperature molten salts, *Chem. Soc. Rev.*, 2014, **43**(10), 3215–3228.

78 B. Deng, J. Tang, X. Mao, Y. Song, H. Zhu and W. Xiao, *et al.*, Kinetic and Thermodynamic Characterization of Enhanced Carbon Dioxide Absorption Process with Lithium Oxide-Containing Ternary Molten Carbonate, *Environ. Sci. Technol.*, 2016, **50**(19), 10588–10595.

79 Z. Chen, B. Deng, K. Du, X. Mao, H. Zhu and W. Xiao, *et al.*, Flue-Gas-Derived Sulfur-Doped Carbon with Enhanced Capacitance, *Adv. Sustainable Syst.*, 2017, **1**(6), 1700047.

80 X. Wang, G. Licht, X. Liu and S. Licht, CO2 Utilization by Electrolytic Splitting to Carbon Nanotubes in Non-Lithiated, Cost-Effective, Molten Carbonate Electrolytes, *Adv. Sustainable Syst.*, 2022, **6**(5), 2100481.

81 B. Deng, M. Gao, R. Yu, X. Mao, R. Jiang and D. Wang, Critical operating conditions for enhanced energy-efficient molten salt CO2 capture and electrolytic utilization as durable looping applications, *Appl. Energy*, 2019, **255**, 113862.

82 E. Sada, S. Katoh, H. Yoshii, I. Takemoto and N. Shiomi, Solubility of carbon dioxide in molten alkali halides and nitrates and their binary mixtures, *J. Chem. Eng. Data*, 1981, **26**(3), 279–281.

83 G. A. Mutch, L. Qu, G. Triantafyllou, W. Xing, M. L. Fontaine and I. S. Metcalfe, Supported molten-salt membranes for carbon dioxide permeation, *J. Mater. Chem. A*, 2019, **7**(21), 12951–12973.

84 S. Wang, F. Zhang, X. Liu and L. Zhang, CaO solubility and activity coefficient in molten salts CaCl2–x (x=0, NaCl, KCl, SrCl2, BaCl2 and LiCl), *Thermochim. Acta*, 2008, **470**(1), 105–107.

85 N. Díez, A. B. Fuertes and M. Sevilla, Molten salt strategies towards carbon materials for energy storage and conversion, *Energy Stor. Mater.*, 2021, **38**, 50–69.

86 K. S. P. Karunadasa, C. H. Manoratne, H. M. T. G. A. Pitawala and R. M. G. Rajapakse, Thermal decomposition of calcium carbonate (calcite polymorph) as examined by in-situ high-temperature X-ray powder diffraction, *J. Phys. Chem. Solids*, 2019, **134**, 21–28.

87 Y. Kanai, K. Fukunaga, K. Terasaka and S. Fujioka, Mass transfer in molten salt and suspended molten salt in bubble column, *Chem. Eng. Sci.*, 2013, **100**, 153–159.

88 D. Peeters, D. Moyaux and P. Claes, Solubility and solvation of carbon dioxide in the molten Li2CO3/Na2CO3/K2CO3 (43.5:31.5:25.0 mol-%) eutectic mixture at 973 K. II. Theoretical Part, *Eur. J. Inorg. Chem.*, 1999, **3**(4), 589–592.

89 P. Claes, D. Moyaux and D. Peeters, Solubility and Solvation of Carbon Dioxide in the Molten Li2CO3/NaCO3/K2CO3 (43.5:31.5:25.0 mol-%) Eutectic Mixture at 973 K I. Experimental Part, *Eur. J. Inorg. Chem.*, 1999, **3**, 583–588.

90 Y. Yu, Z. Li, W. Zhang, W. Li, D. Ji and Y. Liu, *et al.*, Effect of BaCO3 addition on the CO2-derived carbon deposition in molten carbonates electrolyzer, *New J. Chem.*, 2018, **42**(2), 1208–1215.

91 H. Wu, Z. Li, D. Ji, Y. Liu, L. Li and D. Yuan, *et al.*, One-pot synthesis of nanostructured carbon materials from carbon dioxide via electrolysis in molten carbonate salts, *Carbon*, 2016, **106**, 208–217.

92 J. Ren, F. F. Li, J. Lau, L. González-Urbina and S. Licht, One-Pot Synthesis of Carbon Nanofibers from CO2, *Nano Lett.*, 2015, **15**(9), 6142–6148.

93 X. Hu, W. Deng, Z. Shi, Z. Wang, B. Gao and Z. Wang, Solubility of CO2 in Molten Li2O–LiCl System: A Raman Spectroscopy Study, *J. Chem. Eng. Data*, 2019, **64**(1), 202–210.

94 T. Kikuchi, R. Ishida, S. Natsui, T. Kumagai, I. Ogino and N. Sakaguchi, *et al.*, Carbon nanotube synthesis via the calciothermic reduction of carbon dioxide with iron additives, *ECS Solid State Lett.*, 2015, **4**(9), M19–M22.

95 W. Weng, B. Jiang, Z. Wang and W. Xiao, In situ electrochemical conversion of CO2 in molten salts to advanced energy materials with reduced carbon emissions, *Sci. Adv.*, 2020, **6**(9), 2–9.

96 X. Wang, X. Liu, G. Licht, B. Wang and S. Licht, Exploration of alkali cation variation on the synthesis of carbon nanotubes by electrolysis of CO2 in molten carbonates, *J. CO2 Util.*, 2019, **34**, 303–312.

97 G. Dey, J. Ren, T. El-Ghazawi and S. Licht, How does an amalgamated Ni cathode affect carbon nanotube growth? A density functional theory study, *RSC Adv.*, 2016, **6**(32), 27191–27196.

98 I. A. Novoselova, N. F. Oliinyk, S. V. Volkov, A. A. Konchits, I. B. Yanchuk and V. S. Yefanov, *et al.*, Electrolytic synthesis of carbon nanotubes from carbon dioxide in molten salts and their characterization, *Phys. E*, 2008, **40**(7), 2231–2237.

99 Q. Song, Q. Xu, X. Shang, Z. Ning, Y. Qi and K. Yu, Electrochemical Preparation of a Carbon/Cr-O-C Bilayer Film on Stainless Steel in Molten LiCl-KCl-K 2 CO 3, *J. Electrochem. Soc.*, 2015, **162**(1), D82–D85.

100 L. Hu, Y. Song, S. Jiao, Y. Liu, J. Ge and H. Jiao, *et al.*, Direct Conversion of Greenhouse Gas CO2 into Graphene via Molten Salts Electrolysis, *ChemSusChem*, 2016, **9**(6), 588–594.

101 A. Douglas, R. Carter, M. Li and C. L. Pint, Toward Small-Diameter Carbon Nanotubes Synthesized from Captured Carbon Dioxide: Critical Role of Catalyst Coarsening, *ACS Appl. Mater. Interfaces*, 2018, **10**(22), 19010–19018.

102 Y. Chen, Q. Xu, Q. Song, H. Li, Z. Ning and X. Lu, *et al.*, Electrochemistry of acetylide anion and anodic formation of carbon films in a LiCl-KCl-CaCl2-CaC2 melt, *Electrochem. Commun.*, 2016, **64**, 1–4.

103 H. Yin, L. Gao, H. Zhu, X. Mao, F. Gan and D. Wang, On the development of metallic inert anode for molten CaCl2–CaO System, *Electrochim. Acta*, 2011, **56**(9), 3296–3302.

104 J. Ge, J. Wang, J. Cheng and S. Jiao, Electrochemical Conversion of CO 2 in Molten CaCl 2 -LiCl-CaO Utilizing a Low-Cost (1- x)CaTiO 3 - x Ni Inert Anode, *J. Electrochem. Soc.*, 2016, **163**(8), E230–E234.

105 Y. Chen, M. Wang, J. Zhang, J. Tu, J. Ge and S. Jiao, Green and sustainable molten salt electrochemistry for the conversion of secondary carbon pollutants to advanced carbon materials, *J. Mater. Chem. A*, 2021, **9**(25), 14119–14146.

106 L. Hu, Y. Song, J. Ge, J. Zhu and S. Jiao, Capture and electrochemical conversion of CO2 to ultrathin graphite sheets in CaCl2-based melts, *J. Mater. Chem. A*, 2015, **3**(42), 21211–21218.

107 L. Li, Z. Shi, B. Gao, J. Xu, X. Hu and Z. Wang, Electrochemical Behavior of Carbonate Ion in the LiF–NaF–Li2CO3 System, *Electrochemistry*, 2014, **82**(12), 1072–1077.

108 B. Kaplan, H. Groult, A. Barhoun, F. Lantelme, T. Nakajima and V. Gupta, *et al.*, Synthesis and Structural Characterization of Carbon Powder by Electrolytic Reduction of Molten Li_2CO_3-Na_2CO_3-K_2CO_3, *J. Electrochem. Soc.*, 2002, **149**(5), D72.

109 A. R. Kamali, Nanocatalytic conversion of CO2 into nanodiamonds, *Carbon*, 2017, **123**, 205–215.

110 U. Arachchige and M. Melaaen, Aspen Plus Simulation of CO2 Removal from Coal and Gas Fired Power Plants, *Energy Procedia*, 2012, **23**, 391–399.

111 N. Otsuka, 1.18 - Fireside Corrosion, in *Shreir's Corrosion*, ed. B. Cottis, M. Graham, R. Lindsay, S. Lyon, T. Richardson and D. Scantlebury, *et al.*,. Elsevier, Oxford, 2010, [cited 2022 Jun 23], pp. 457–481, Available from: **https://www.sciencedirect.com/science/article/pii/B978044452787500192X**.

112 H. Wu, Y. Liu, D. Ji, Z. Li, G. Yi and D. Yuan, *et al.*, Renewable and high efficient syngas production from carbon dioxide and water through solar energy assisted electrolysis in eutectic molten salts, *J. Power Sources*, 2017, **362**, 92–104.

113 V. Kaplan, E. Wachtel and I. Lubomirsky, CO 2 to CO Electrochemical Conversion in Molten Li 2 CO 3 Is Stable with Respect to Sulfur Contamination, *J. Electrochem. Soc.*, 2014, **161**(1), F54–F57.

114 Z. Chen, Y. Gu, L. Hu, W. Xiao, X. Mao and H. Zhu, *et al.*, Synthesis of nanostructured graphite: Via molten salt reduction of CO2 and SO2 at a relatively low temperature, *J. Mater. Chem. A*, 2017, **5**(39), 20603–20607.

115 X. Chen, H. Zhao, J. Qu, D. Tang, Z. Zhao and H. Xie, *et al.*, A molten calcium carbonate mediator for the electrochemical conversion and absorption of carbon dioxide, *Green Chem.*, 2020, **22**(22), 7946–7954.